Current Status of Theory of Nuclear Quadrupole Interaction in Metallic Systems*

T. P. Das
Department of Physics, State University of New York at Albany, Albany, New York, 12222, USA

P. C. Schmidt
Institut für Physikalische Chemie, Physikalische Chemie III, Technische Hochschule Darmstadt, West Germany

Z. Naturforsch. **41 a**, 47–77 (1986); received November 30, 1985

This paper deals with the current status of understanding of the factors that determine the origin of nuclear quadrupole interactions in metallic systems. The major emphasis is on pure metals in which there is currently better understanding of the origin of the electric field gradient (EFG) at the nuclear sites. The procedures for the determination of the electron densities that lead to the electronic contributions to the EFG's is discussed as well as the quantitative procedures for incorporation of antishielding effects. The nature of agreement between theory and experiment is examined by considering the hexagonal close packed metals beryllium, magnesium, zinc and cadmium. The sensitiveness of the calculated EFG to the procedure used for obtaining electron densities is discussed in beryllium using orthogonalized plane wave and augmented plane wave procedures. The nature of agreement between theory and experiment currently attainable for semi-metals and semiconductors is discussed. The bearing of some of the results in these latter systems by procedures dealing with clusters of atoms to simulate the infinite solid on the future of such procedures for imperfect systems and surfaces is commented upon. A brief discussion is presented about the various possible contributors to the temperature dependence of EFG's in pure metals and comparison is made between theory and experiment for zinc and cadmium. The factors that can contribute to the EFG's in imperfect metallic systems, including alloys, at both host and impurity nuclei are discussed, and some of these factors are illustrated by considering two examples of these systems, EFG's at host Al and Cu nuclei due to mu mesons introduced in the metal and at impurity nuclei in alloys involving cadmium metal host. The concluding section discusses directions in which further efforts are needed to improve our theoretical understanding of both pure metals and imperfect metallic systems.

1. Introduction

This conference provides an appropriate forum to discuss the current status of understanding of the nuclear quadrupole interaction (NQI) in metallic systems since it has substantial representation from both scientists using conventional resonance techniques [1, 2] as well as those using radiative techniques such as perturbed angular correlation [3], β-decay NMR [4], oriented Nuclei NMR [5] and Mössbauer Effect [6]. The field of NQI in metallic systems is perhaps one of the best examples where the two types of techniques have complemented each other very well, the radiative techniques having allowed one to study nuclear quadrupole effects at the impurity sites themselves in alloy systems while the conventional resonance techniques have provided valuable information on these effects at host nuclei adjacent to the impurity ions.

In this review we shall discuss the various mechanisms that can contribute to the EFG's at nuclei in pure metals and imperfect metal systems such as systems involving substitutional and interstitial impurity atoms and ions, vacancies, and atoms at surfaces.

As examples of the applications of the theoretical methods that have been developed, we shall primarily refer to systems that we have studied. However, references will be made to other theoretical investigations at the appropriate places.

The first part of this article will deal with pure metals and the second part with imperfect metallic systems.

Reprint requests to Dr. P. C. Schmidt, Physikalische Chemie III, Technische Hochschule Darmstadt, Petersenstr. 20, D-6100 Darmstadt, West Germany (for USA to TPD).

* Presented at the VIIIth International Symposium on Nuclear Quadrupole Resonance Spectroscopy, Darmstadt, July 22–26, 1985.

0340-4811 / 86 / 0100-0047 $ 01.30/0. – Please order a reprint rather than making your own copy.

2. Origin of Nuclear Quadrupole Interaction in Pure Metals

All experimental techniques [1–6] aimed at studying the NQI attempt to measure the quadrupole coupling constant e^2qQ and the asymmetry parameter η, and in those cases where they cannot be shown to vanish from symmetry considerations [7] one also aims at obtaining the directions of the principal axes. Considering the contributions from both the ionic charges in the lattice and the valence electrons [8], the EFG q, representing the maximum component in the principal axis system is given by

$$q = \sum_s \zeta_s e \left(\frac{3\cos^2 \vartheta_s - 1}{r_s^3} \right) (1 - \gamma_\infty) - \int e\varrho(\boldsymbol{r}) (1 - \gamma(r)) \cdot \frac{3\cos^2 \vartheta - 1}{r^3} \, d\tau , \quad (1)$$

where $\zeta_s e$ is the charge on the sth ion, ϑ_s is the angle between the line joining the sth ion to the central one (containing the nucleus under study) and the z-axis, and r_s is the length of the line. $\varrho(\boldsymbol{r})$ is the electron density due to the conduction electrons at a point described by the radius vector $\boldsymbol{r}$ with respect to the nucleus of interest and r and ϑ are, the length and angle with respect to the z-axis of $\boldsymbol{r}$. The quantity γ_∞ is the Sternheimer antishielding factor [9] for the ions in the lattice appropriate for the EFG due to a totally external charge and $\gamma(r)$ is the antishielding function [10] which depends on the distance of the conduction electron from the nucleus. For r going to infinity, $\gamma(r)$ reduces to γ_∞. For intermediate distances $\gamma(r)$ must include exchange effects associated with the indistinguishability of conduction and core electrons when their wave functions overlap.

Thus, for a quantitative understanding of the nuclear quadrupole coupling constants (NQCC) in metals, the following are needed:

a) Knowledge of the nuclear quadrupole moments, Q, of the nucleus under study.
b) Knowledge of lattice structure of the metal, which one needs for obtaining the positions of the ions.
c) Accurate knowledge of charge distributions due to conduction electrons.
d) Appropriate antishielding effects as represented by the Sternheimer antishielding parameter γ_∞ and the antishielding function $\gamma(r)$.

These questions are discussed in separate sections of the first part and are followed by sections dealing with the results of calculation of the absolute values of the EFG's in hexagonal close packed metals, a comparison of the EFG's in metals by two different procedures, EFG's in semi-metals and semiconductors and the temperature dependence of the EFG.

2.1. Determination of nuclear quadrupole moments

A number of methods have been utilized for accurate determination of Q, since their discovery by Schüler and Schmidt [11]. Among the ones most commonly used are atomic beam studies [12] involving transitions between nuclear Zeeman levels or more recently, studies at optical transitions using laser techniques [13]. These measurements provide the value of the quadrupole coupling constant e^2qQ for a particular atomic state, q being the EFG at the nucleus for this state. Careful calculations [14] of q then provide accurate values of Q. The various contributions to q consist of the direct contribution from the one or more valence electrons, the shielding or antishielding factor γ_A [15] due to the perturbation of the core electrons by the valence electrons and many-body effects [14] involving dynamic interactions between the valence and core electrons both among themselves and between each other. The shielding effects have been studied [16] for a number of atomic systems by the differential equation procedure of Sternheimer [17] as well as its variational counterpart [18]. Also the many-body perturbation theoretic technique [19] has been utilized [14] in some cases, and in a number of these cases, very good agreement is found [14] for the direct contribution to γ_A with the results of the Sternheimer procedure [17]. Many-body and consistency effects on γ_A have been studied [20] in a number of cases by the many-body perturbation technique. While consistency effects are found to be significant many-body effects have been found to be relatively small for γ_A. A conservative estimate of the accuracy involved in the evaluation of various contributions to γ_A suggests [20] a net confidence limit of 20% and remembering the fact that γ_A is usually of the order of 0.1, this means an overall confidence limit of 1% in the total EFG. Thus the net accuracy of the quadrupole moments are basically determined [21] by that of the experimentally

measured NQCC's. These methods can be applied to both ground and excited atomic states. Examples of the former, important for NQI studies in metals, are ^{27}Al, ^{71}Ga, and ^{113,115}In. Typical examples of systems where one has to study excited atomic states because the ground states are spherically symmetric are the alkali atom nuclei for which excited atomic states involving the valence electrons in p-states are studied [22]. The nuclei of second group atoms also belong to this category and for ^{9}Be, ^{25}Mg, and ^{67}Zn the ^{3}P excited states involving the two valence electrons in s and p states have been studied [23] to obtain the NQCC's.

For some nuclei, where for particular reasons it is not possible to measure the NQCC in a non-spherical atomic state, one resorts to studies in molecular systems, either by molecular beam [24] or microwave [25] techniques or by perturbed angular correlation (PAC) [26] or Mössbauer effect (ME) [27] studies in molecules trapped in solid-state systems, often in a rare gas matrix. Examples of nuclei of these types are the excited state of ^{19}F nucleus [26] which has a spin of $I = 5/2$ and hence a finite Q and the important Mössbauer active state of the iron [28] nucleus ^{57m}Fe for which molecular Hartree-Fock (HF) calculations [29, 30] combined with PAC and ME quadrupole coupling data have provided the Q's of these nuclei. Another example is the ^{14}N nucleus, for which Q has been obtained from molecular calculations [31]. A recent relativistic many-body perturbation theoretic investigation [32], on the ground $2p^3$ configuration of nitrogen atom, which is not strictly spherical in relativistic theory, has verified the value of Q from the molecular calculations.

Lastly, there is the method involving muonic atoms [33] which, as mentioned by Professor Brix [34] in his lecture at this conference, is being increasingly used for making accurate measurements of quadrupole moments. In this method, the NQI due to a negative muon is measured when it is in a non-s state. Since the muonium moves very close to the nucleus, its orbit can be considered as a hydrogenic one in the field of the entire nuclear charge. The EFG due to it at the nucleus can then be calculated exactly, yielding an accurate value of Q. There is one uncertainty in the determination of Q by this method that one may be concerned about. This has to do with the fact that the muon would be expected to spend substantial time within the nuclear radius and thus perturb it and thereby change the Q itself that one is attempting to measure. However, this is expected to be an important problem more for magnetic hyperfine interaction studies where one deals with s-states of the muon, rather than for the quadrupole interaction studies where one deals with p, d and other non-s states for which there is less penetration inside the nucleus. Nevertheless it would be helpful to make comparisons between Q's for the same nuclei determined from muonic [33] and electronic [34] NQI in a number of cases to assess the accuracy of the Q obtained from the two types of interactions.

2.2. *Lattice structure*

For pure metals, a knowledge of the positions of the ions in the lattice, necessary for both the evaluation of the lattice sum in (1) and the study of the band structure and wave-functions to obtain the $\varrho(\boldsymbol{r})$ in the second term in (1), does not present any special difficulties as it does for the case of imperfect metallic systems. One needs an accurate determination of the crystal structure from X-ray diffraction techniques and accurate measurements of crystal structure are available for most pure metals. For the analysis of the temperature dependence of the EFG's in metal, one needs [35] a knowledge of the crystal structure as a function of temperature, which is less widely available.

2.3. *Electron density distribution in metals*

One can in principle obtain the electron density function $\varrho(\boldsymbol{r})$ in the second term in (1) by electron diffraction techniques. But data from measurements of this type are presently not widely available, or are not accurate enough, to carry out the integration in (1) and obtain the electronic contribution to the EFG. One has therefore to resort to theoretical procedures to determine $\varrho(\boldsymbol{r})$ by obtaining the electronic wavefunctions in the metals. There are a number of procedures that have been developed in the literature for determination of band structure and wave-functions. We shall touch briefly on a few of them that have been used in the evaluation of electron densities for study of magnetic and nuclear quadrupole hyperfine interaction properties. However, before proceeding on to this, we would like to point out that approximate procedures based on the Thomas-Fermi model are being applied [36] with

increasing sophistication to obtain the electronic contributions to the EFG. The reader is referred to the most recent paper on the subject and references therein [36].

2.3.1. Tight-binding procedure

The tight-binding (TB) procedure [37] is best suited for systems which have rather narrow bands, indicating strong intra-atomic binding and relatively weak interatomic bonding. Thus, it would be applicable to ionic crystals as well as systems like gallium metal or graphite. The electronic wave-function in this procedure is taken in the form

$$\psi_{\boldsymbol{k}}(\boldsymbol{r}) = \sum_{s} e^{i\boldsymbol{k}\cdot\boldsymbol{r}_s}\, \Phi(\boldsymbol{r}-\boldsymbol{r}_s)\,, \tag{2}$$

where s refers to the various lattice points which occur as a periodic array. The function $\Phi(\boldsymbol{r}-\boldsymbol{r}_s)$ is expanded in the variational form:

$$\Phi(\boldsymbol{r}-\boldsymbol{r}_s) = \sum_{\mu} c_\mu \chi_\mu(\boldsymbol{r}-\boldsymbol{r}_s)\,. \tag{3}$$

The $\chi_\mu(\boldsymbol{r}-\boldsymbol{r}_s)$ refer to valence electron atomic functions at the lattice sites, the coefficients c_μ being determined variationally. The potential is often taken as a sum over a periodic array of atomic-like potentials but one can also take general potentials more representative of the solid and additionally consider the c_μ as function of $\boldsymbol{k}$ which can make the procedure adaptable to systems in which the bands are not too narrow and the valence electrons are significantly delocalized.

2.3.2. Orthogonalized plane-wave procedure

This procedure [38] is more general in scope and is in principle applicable to both broad and narrow bands, somewhat more suited to the former. The Bloch wave-functions in this case are taken in the form

$$\psi_{\boldsymbol{k}}(\boldsymbol{r}) = \sum_{\boldsymbol{g}_i} c_i \mathrm{OPW}(\boldsymbol{k}_i, \boldsymbol{r}); \quad \boldsymbol{k}_i = \boldsymbol{k} + \boldsymbol{g}_i\,, \tag{4}$$

where the $\boldsymbol{g}_i$ refer to reciprocal lattice vectors, c_i are variational parameters, and the $\mathrm{OPW}(\boldsymbol{k}_i, \boldsymbol{r})$ are given by

$$\mathrm{OPW}(\boldsymbol{k}_i, \boldsymbol{r}) = N_{\boldsymbol{k}_i}(\mathrm{PW}(\boldsymbol{k}_i, \boldsymbol{r}) - \sum_{c} b_{\boldsymbol{k}_i, c}\, \psi_{c, \boldsymbol{k}_i}(\boldsymbol{r}) \tag{5}$$

with the $\psi_{c,\boldsymbol{k}_i}(r)$ referring to tight-binding Bloch wave-functions corresponding to the core state c, $b_{\boldsymbol{k}_i, c}$ being determined by the orthogonality condition

$$\langle \mathrm{OPW}(\boldsymbol{k}_i, \boldsymbol{r}) \,|\, \psi_{c,\boldsymbol{k}_i}(\boldsymbol{r})\rangle = 0\,, \tag{6}$$

which leads to

$$b_{\boldsymbol{k}_i, c} = \langle \mathrm{PW}(\boldsymbol{k}_i, \boldsymbol{r}) \,|\, \psi_{c,\boldsymbol{k}_i}(\boldsymbol{r})\rangle\,. \tag{7}$$

The plane-wave functions being given by

$$\mathrm{PW}(\boldsymbol{k}_i, \boldsymbol{r}) = e^{i\boldsymbol{k}_i\cdot\boldsymbol{r}}/\sqrt{N\Omega} \tag{8}$$

with N representing the number of atoms in the solid and Ω, the Wigner-Seitz volume or the volume per atom. The quantity $N_{\boldsymbol{k}_i}$ represents the normalization factor for the function $\mathrm{OPW}(\boldsymbol{k}_i, \boldsymbol{r})$ and is given by

$$N_{\boldsymbol{k}_i} = \frac{1}{\sqrt{1 - \sum_{c} |b_{\boldsymbol{k}_i, c}|^2}}\,, \tag{9}$$

assuming that the core states on different ions do not overlap. The parameters c_i are determined by the usual variational procedure, leading to the linear equations

$$\sum_{i} c_i (H_{i,j} - E_{\boldsymbol{k}} S_{i,j}) = 0\,, \tag{10}$$

where $H_{i,j}$ are the matrix elements of the Hamiltonian

$$H_{i,j} = \langle \mathrm{OPW}(\boldsymbol{k}_i, \boldsymbol{r}) \,|\, \hat{H}(\boldsymbol{r}) \,|\, \mathrm{OPW}(\boldsymbol{k}_j, \boldsymbol{r})\rangle \tag{11}$$

and $S_{i,j}$ the overlap integrals between OPW functions,

$$S_{i,j} = \langle \mathrm{OPW}(\boldsymbol{k}_i, \boldsymbol{r}) \,|\, \mathrm{OPW}(\boldsymbol{k}_j, \boldsymbol{r})\rangle\,. \tag{12}$$

In principle, one should use the rigorous Hamiltonian for the many-electron system, namely

$$\hat{H} = \sum_{n}\left[-\frac{h^2}{2m_e}\nabla_n^2 - \sum_{s}\frac{\zeta_s e^2}{|\boldsymbol{r}_n - \boldsymbol{r}_s|} + \sum_{n'>n}\frac{e^2}{r_{nn'}}\right], \tag{13}$$

where $\zeta_s e$ represents the charge on the ion in the metal at site s, but in practice, for reducing computational efforts one uses

$$\hat{H} = \sum_{n}\hat{H}(n) = -\sum_{n}\frac{\hbar^2}{2m_e}\nabla_n^2 + \sum_{s,n} V(|\boldsymbol{r}_n - \boldsymbol{r}_s|)\,, \tag{14}$$

where $V(|\boldsymbol{r}_n - \boldsymbol{r}_s|)$ is a one-electron potential centered at the lattice site s, involving the nuclear potential and the Coulomb and exchange potentials associated with the interaction between the conduction and

core electrons and the conduction electrons themselves, with the exchange potential approximated to be local, either in terms of the statistical exchange approximations [39] or something closer [40] to the HF approximation especially for the core-conduction exchange. For reasonably good metals with the conduction electrons fairly delocalized, the inclusion of 20 to 25 basis states in the summation in (4) is adequate, the exact number depending on the particular $\boldsymbol{k}$, especially its symmetry in reciprocal space.

2.3.3. The augmented plane wave procedure

The Augmented Plane Wave (APW) procedure [41] is based on the expectation that in a metallic system, there will be regions in space where the conduction electron is close to free-electron like, while in the ion-core regions, the conduction electron wave-functions will have atomic-like character. While in the OPW procedure, this atomic-like character is incorporated through the use of basis functions involving plane-waves orthogonalized to the core functions, in the APW procedure, the atomic-like character in the core region is included through the use of solutions of the Schrödinger (non-relativistic) or Dirac (relativistic) equations obtained for this region using the appropriate conduction electron potential.

The potential in the APW approximation is considered to be atomic-like inside a sphere surrounding the nucleus of radius R_s, while outside it is assumed to be uniform. The arrangement of these spheres and uniform regions is shown schematically in Fig. 1 and it is easy to understand why the name muffin-tin potential is given to this choice of potential. The procedure for obtaining wave-functions in the APW approximation proceeds as follows. The first step is to solve for atomic-like states inside the muffin sphere for a set of different values of the energy E, which is expected to span the occupied as well as empty band states of interest, the wave-functions being expressed in the form

$$\psi_{l,m}(\boldsymbol{r}, E) = Y_{l,m}(\vartheta, \varphi)\, R_l(r, E)\,. \tag{15}$$

The second step involves preparing basis functions for carrying out variational calculations which are given by

$$(\Phi_i)^E_{\text{inside}} = \sum_{l,m} Y_{l,m}(\vartheta, \varphi)\, R_l(r, E)\, A_{l,m}(\boldsymbol{k}_i)\,, \tag{16}$$

$$(\Phi_i)^E_{\text{outside}} = e^{i\boldsymbol{k}_i \cdot \boldsymbol{r}}, \tag{17}$$

where $\boldsymbol{k}_i = \boldsymbol{k} + \boldsymbol{g}_i$, with the $A_{lm}(\boldsymbol{k}_i)$ obtained by matching the partial waves in (17) for various l and m with those in (16). One then uses a variational function of the form

$$\psi_{\boldsymbol{k}}(\boldsymbol{r}) = \sum_i c_i \Phi_i^E(\boldsymbol{r}) \tag{18}$$

with the c_i satisfying the linear equations

$$\sum_i c_i (H_{ij} - E S_{ij}) = 0\,, \tag{19}$$

where

$$H_{ij} = \langle \Phi_i^E \,|\, H \,|\, \Phi_j^E \rangle + F_{ij} \tag{20}$$

and

$$S_{ij} = \langle \Phi_i^E \,|\, \Phi_j^E \rangle\,,$$

leading to the secular equation

$$\text{Det}\,|\, H_{ij} - E S_{ij} \,| = 0\,. \tag{21}$$

F_{ij} are surface integrals taken into account the discontinuous slope of Φ_i^E for $r = R_s$ [41]. To solve (21) for the values of E, one looks for the zeros of the determinant by an interpolation procedure. This process is carried out for each $\boldsymbol{k}$ in the grid chosen in the Brillouin zone for obtaining the energy bands (and wave functions) as a function of $\boldsymbol{k}$ and provides the band structure.

It should be noted that this procedure does not have to use a uniform potential outside the muffin sphere [42]. One can use the latter idealized approximation for preparation of the basis functions Φ_i. For obtaining H_{ij} in (20) one can subsequently use the actual potentials involving both radial variation outwards with respect to the muffin center as origin, as well as non-central character represented by angular variation of the potential both within and outside the sphere. If the deviation from the idealized potential is not too strong, one can also apply a perturbation procedure using the energy bands and wave-functions for the idealized potential to take account of the actual potential and the idealized potential. A perturbation procedure has been used [43] recently for beryllium to take account of the difference between HF exchange [40] and the Slater type statistical approximation [39] to it.

2.3.4. Hybridized tight binding and orthogonalized plane wave procedure

A procedure that would be particularly suited for EFG studies but has not yet been used extensively

for this purpose is a procedure [44] involving a combination of TB and OPW functions. For this procedure, the wave function has the form [44]

$$\psi_{\boldsymbol{k}}(\boldsymbol{k}) = \sum_{\boldsymbol{g}_i} c_{\boldsymbol{k}+\boldsymbol{g}_i} \mathrm{OPW}(\boldsymbol{k}+\boldsymbol{g}_i, \boldsymbol{r}) + \sum_s \sum_\mu e^{i\boldsymbol{k}\cdot\boldsymbol{r}_s} c_{\boldsymbol{k},\mu}\, \chi_\mu(\boldsymbol{r}-\boldsymbol{r}_s)\,, \qquad (22)$$

where the TB and OPW functions are given by (3) and (5) with the quantities $c_{\boldsymbol{k}+\boldsymbol{g}_i}$ and $c_{\boldsymbol{k},\mu}$ to be obtained by the use of the variation principle. This procedure allows good flexibility to treat both narrow and broad bands and also to obtain a good description of both the regions between the cores which are important for their influence on the band structure and the region near the nucleus which is important for the EFG at the nucleus. This procedure has so far been applied to study band-structures and hyperfine and other properties of the ferromagnetic metals [44] iron, cobalt and nickel, using the exact Hamiltonian (13). In these investigations a SCF-HF procedure with explicit incorporation of some aspects of many-body effects was utilized for determining the band structure and wave-functions.

2.3.5. Pseudopotential treatments

A somewhat less time-consuming procedure for determination of conduction electron wave-functions involves the pseudopotential approach [45, 46]. In this approach one employs [46] a linear combination of plane waves, obtained using a pseudopotential replacing the actual potential, and then replaces the plane waves by OPW functions. Thus, one uses the equation

$$\left(-\frac{\hbar^2}{2m_e}\nabla^2 + V_{\mathrm{pseudo}}\right)\Phi_{\boldsymbol{k}} = E_{\boldsymbol{k}}\Phi_{\boldsymbol{k}}\,, \qquad (23)$$

where $\Phi_{\boldsymbol{k}}$ is a pseudofunction represented by a linear combination of plane-waves in the form

$$\Phi_{\boldsymbol{k}} = \sum_i c_i \mathrm{PW}(\boldsymbol{k}+\boldsymbol{g}_i, \boldsymbol{r}) \qquad (24)$$

with PW ($\boldsymbol{k}$, r) given by (8) and the c_i to be obtained by solving (23) variationally. With the pseudopotential V_{pseudo}, one expects [45] to obtain the same $E_{\boldsymbol{k}}$ by solving (23) for $\Phi_{\boldsymbol{k}}$ as one would get by solving the corresponding Schrödinger equation for the actual potential and the actual eigenfunction for the particular $\boldsymbol{k}$ and band under study.

The pseudopotential is obtained in different ways [45], either by fitting to experimental information [47] available about the nature of the Fermi surface or by ab initio calculations [48]. The various procedures used to determine pseudopotentials, the assumptions involved in deriving them, and their relative accuracies, have been discussed extensively at various places in the literature [45, 49] and the reader should refer to them. Once the pseudo wave-functions in (24) are determined one can obtain [46] the actual wave-functions from it by replacing the PW $(\boldsymbol{k}+\boldsymbol{g}_i, \boldsymbol{r})$ by OPW $(\boldsymbol{k}+\boldsymbol{g}_i, \boldsymbol{r})$ as in (4). This procedure has been used for the evaluation of the conduction electron contributions to EFG's in magnesium, zinc, and cadmium [50–53] the results for which will be discussed in Section 2.5.

2.4. Incorporation of antishielding effects in the evaluation of electric field gradients in metals

The next important topic one has to discuss for the study of EFG's in pure metals is the quantitative incorporation of antishielding effects [9, 10, 14–18, 20] in the electronic and lattice contributions to the EFG as indicated in (1). We consider first the question of antishielding effects associated with the conduction electrons. Since the conduction electron distribution penetrates the ion cores, one cannot use the Sternheimer antishielding factor [9] appropriate for a charge totally external to the core electrons. On the other hand, the charge distribution is not internal enough to use the atomic type Sternheimer antishielding factor [15, 16] appropriate for the field gradient produced by a valence electron. One has therefore to make use of an antishielding function [10] $\gamma(r)$ which varies with the position of the conduction electron as indicated in (1). Antishielding functions $\gamma(r)$ have been calculated in the literature [54] for a number of ions placing a point charge producing the EFG at different distances from the nuclear quadrupole moment, Q. As mentioned earlier, the use of a function $\gamma(r)$ obtained in this way would not include exchange effects between the conduction and core electrons when they overlap. A procedure which would incorporate such exchange effects explicitly and would replace the integration over $\gamma(r)$ in (1) has been used in the literature [55] and we shall describe it briefly. The first step in this procedure is to obtain the perturbation $\delta\psi_{Q,c}$ in the core wave functions ψ_c due to

the potential produced by Q. This is done by solving the first order perturbation equation

$$(H_{0,c} - \mathscr{E}_{0,c})\,\delta\psi_{Q,c} = -(H_Q - \delta\mathscr{E}_{Q,c})\,\psi_c\,, \quad (25)$$

where $H_{0,c}$ and $\mathscr{E}_{0,c}$ are the Hamiltonian and energy appropriate for the state ψ_c, H_Q is the perturbation Hamiltonian due to the potential produced by the nuclear quadrupole moment, namely

$$H_Q = \frac{e^2 Q\,(3\cos^2\vartheta - 1)}{r^3}\,, \quad (26)$$

and $\delta\mathscr{E}_{Q,c}$ is the first-order perturbation energy for the core state c given by

$$\delta\mathscr{E}_{Q,c} = \langle\psi_c|\,H_Q\,|\psi_c\rangle\,. \quad (27)$$

The next step in the procedure is to calculate the energy of interaction between the perturbed core state and the conduction electrons to terms linear in Q. This perturbation energy which can be considered as of second order, involving one order in H_Q and the other in the Coulomb and exchange interactions between the core and conduction electrons will be given by

$$\begin{aligned}\delta^2 E_Q^{\mathrm{el}} &= e^2 Q\,\delta q_{\mathrm{el}}^{\mathrm{ind}} \\ &= 2\sum_{\boldsymbol{k},n}\sum_{c}\int \psi_c^*(1)\,\psi_{\boldsymbol{k},n}^*(2)\,\frac{(1-P_{12})\,e^2}{r_{12}} \\ &\quad\cdot \delta\psi_{Q,c}(1)\,\psi_{\boldsymbol{k},n}(2)\,\mathrm{d}\tau_1\,\mathrm{d}\tau_2\,, \end{aligned} \quad (28)$$

where the operator P_{12} exchanges electrons 1 and 2, the summation over n in (28) referring to the various energy bands which are totally or partially occupied and that over $\boldsymbol{k}$ to all $\boldsymbol{k}$ vectors for each band for which the energy is less than the Fermi energy. Equation (28) gives the induced EFG $\delta q_{\mathrm{el}}^{\mathrm{ind}}$, arising from the core electrons. The total EFG to be used for the conduction electrons (second term in (1)) thus is

$$q_{\mathrm{el}} = q_{\mathrm{el}}^{\mathrm{direct}} + \delta q_{\mathrm{el}}^{\mathrm{ind}}\,, \quad (29)$$

where $q_{\mathrm{el}}^{\mathrm{direct}}$ is the unshielded value of the EFG due to the conduction electrons, namely,

$$q_{\mathrm{el}}^{\mathrm{direct}} = \sum_{\boldsymbol{k},n}\int \psi_{\boldsymbol{k},n}^*(\boldsymbol{r})\,\frac{3\cos^2\vartheta - 1}{r^3}\,\psi_{\boldsymbol{k},n}(\boldsymbol{r})\,\mathrm{d}\tau\,. \quad (30)$$

It is interesting [55] to examine the effective antishielding factor $\gamma_{\mathrm{eff}} = \delta q_{q_{\mathrm{el}}}^{\mathrm{ind}}/q_{\mathrm{el}}^{\mathrm{direct}}$ experienced by the EFG's associated with different components of the conduction electron density. Thus, considering the conduction electron wave-functions given by (4) and (5) in the OPW formalism [38], we can separate $\varrho(\boldsymbol{r}) = \sum_{\boldsymbol{k},n} |\psi_{\boldsymbol{k},n}(\boldsymbol{r})|^2$ into three components, PW-PW, involving only the plane-wave components of the wave functions, PW-TB, involving the cross term composed of the product of PW and TB components and TB-TB, composed of only the TB components. For the EFG's due to these three components, taking the ratio of the corresponding δq^{ind} and $q_{\mathrm{el}}^{\mathrm{direct}}$ occurring in (28) and (30), it has been found [55] that both for zinc and cadmium

$$\begin{aligned}(\gamma_{\mathrm{eff}})_{\text{PW-PW}} &\approx 0.65\,\gamma_\infty\,; \\ (\gamma_{\mathrm{eff}})_{\text{PW-TB}} &\approx 0.02\,\gamma_\infty\,; \\ (\gamma_{\mathrm{eff}})_{\text{TB-TB}} &\approx 0.06\,\gamma_\infty\,. \end{aligned} \quad (31)$$

These results are expected from physical considerations since the (PW-PW) component is much more external to the cores than the other components. The size and importance of $(\gamma_{\mathrm{eff}})_{\text{PW-PW}}$ has significant bearing on an empirical relationship [56] derived for EFG's at impurity sites in alloy systems involving noncubic hosts, as will be discussed in the second part of this paper.

For the contributions to the EFG from the charges on the ions, represented by the first term in (1), the use of γ_∞ should be quite justified since the ion cores are not expected to overlap significantly or have their charge distribution significantly different in the metal as compared to the ions. But, if one wants to be careful about this point, one can also carry out a calculation similar to that [55] for the antishielding effect on conduction electron contribution to the EFG, using

$$q_{\mathrm{ion}} = q_{\mathrm{ion}}^{\mathrm{direct}} + \delta q_{\mathrm{ion}}^{\mathrm{ind}}\,, \quad (32)$$

$$q_{\mathrm{ion}}^{\mathrm{direct}} = \zeta e\,\frac{3\cos^2\vartheta - 1}{R^3} \quad (33)$$

for a lattice charge ζe whose position vector with respect to the nucleus is $\boldsymbol{R}(R, \vartheta)$, and

$$\begin{aligned}\delta^2 E_Q^{\mathrm{ion}} &= e^2 Q\,\delta q_{\mathrm{ion}}^{\mathrm{ind}} \\ &= 2e^2 Q\int \psi_c^*(\boldsymbol{r})\,\frac{1}{|\boldsymbol{r}-\boldsymbol{R}|}\,\delta\psi_c(\boldsymbol{r})\,\mathrm{d}\tau\,. \end{aligned} \quad (34)$$

The value of $\gamma_{\mathrm{eff}}^{\mathrm{ion}} = \delta q_{\mathrm{ion}}^{\mathrm{ind}}/q_{\mathrm{ion}}^{\mathrm{direct}}$ is expected to depart from γ_∞, if at all, only for the ions which are nearest neighbours to the ion containing the nucleus at which the EFG is being studied.

2.5. Results of calculation of field gradients in hexagonal close packed (group II) metals – comparison with experiment

To illustrate the nature of the various contributions to the EFG and how the results of theory compare with experiment, we shall discuss the situations in the four hexagonal close packed metals beryllium [57], magnesium [58], zinc [59], and cadmium [60]. A few other metals [61] have been investigated in as much detail, but we shall discuss only the four hcp metals because they have similar structures and provide useful insights, when taken together, into the factors influencing the EFG's at the nuclei.

Of these metals, Mg [51] with a c/a ratio of 1.624 is closest to that (1.633) for ideal hexagonal close packing, while Be [51] has a significantly smaller c/a ratio, namely 1.567. On the other hand, Zn and Cd, with the values of c/a as 1.828 and 1.862 respectively [53], are severely distorted compared to the ideal hcp case. The results [57–60] for the lattice, electronic and total contributions to the EFG are tabulated for the four metals in Table 1. The experimental values of the total field gradient eq_{exp} [62–68] are also listed for ready comparison between theory and experiment. These experimental values are obtained from the measured $e^2 q Q$ by dividing by the available Q [69]. For the metals Be [62] and Mg [63], the e^2qQ are obtained from NMR measurements. For Zn, e^2qQ has been obtained from ME [64], NQR [66] and NMR [67] measurements, the coupling constant referring to the ground nuclear state ^{67}Zn with spin $I = 5/2$, the excited nuclear state for Mössbauer measurements having a spin $I = 1/2$ with $Q \equiv 0$. For Cd, the experimental coupling constant is for the excited nuclear state of ^{111}Cd* with $I = 5/2$, from $\beta - \gamma$ perturbed angular correlation (PAC) measurements [68]. For both Zn and Cd, the sign of the coupling constant is known from the Mössbauer and PAC measurements and therefore the experimental value of eq is known. The theoretical electronic contributions to the EFG's in Table 1 were obtained using OPW [57] functions in all four cases, the values for Be and Mg [58] being obtained using wave functions from OPW calculations, while those for Zn [59] and Cd [60] were obtained using OPW functions derived from pseudopotential investigations described in Section 2.3.5.

Table 1. Various contributions to the field-gradients in the hexagonal close packed metals, beryllium through cadmium [a].

Metal	Lattice contribution (eq_{latt})	Electronic contribution (eq_{el})	Total electric field-gradient (eq_{theor})	Experimental value (eq_{exp})
Beryllium	1.97	−2.64	−0.67	1.40 [b]
Magnesium	0.58	1.99	2.47	2.04 [c]
Zinc	−64.40	212.12	147.72	137.9 [d]
				124.0 [e]
				132.2 [f]
				123.6 [g]
Cadmium	−119.60	418.03	299.43	276.1 [h]

[a] All electric field-gradients are expressed in units of 10^{13} esu/cm^3.
[b] Based on NMR measurements, Ref. [62].
[c] Based on NMR measurements, Ref. [63].
[d] Based on Mössbauer measurement, Ref. [64].
[e] Based on Mössbauer measurement, Ref. [65].
[f] Based on NQR measurement, Ref. [66].
[g] Based on NMR measurement, Ref. [67].
[h] Based on $\beta - \gamma$ perturbed angular correlation measurement, Ref. [68].

The lattice contributions in the first column of Table 1 show an interesting trend from Be to Cd, changing from small and positive to large and negative. Part of the increase in magnitude is due to the increasing antishielding effect, γ_∞ being actually small and positive (shielding) for Be^{2+} namely [70] 0.185 and increasing continuously from Mg^{2+} to Cd^{2+} the values for Mg^{2+}, Zn^{2+} and Cd^{2+} being respectively [70] −3.2, −12.7, and −31.9. The change in sign of the lattice contribution, and the rest of the increase in magnitude in going from Mg^{2+} to Cd^{2+} is a consequence of the increase of c/a and can be understood from the theoretical relation [71] derived for the evaluation of the lattice contribution. It is interesting, as has been noted [72] earlier in the literature, that q_{latt} does not go to zero at the ideal [73] hcp ratio $c/a = 1.633$. The electronic contribution also increases with the increase in c/a since the system tends towards stronger departure from cubic symmetry, which is reflected in the nature of the potential and hence in the charge density distribution. Interestingly enough, the sign of the electronic EFG now changes before Mg rather than after, as has been found for q_{latt}. This is not unexpected because of the strong cancellation between individual band contributions for Be and Mg, as will be discussed in Section 2.6. This behaviour also indicates that while the symmetry of the ionic arrangement in the lattice determines if

there is going to be a finite q_{latt}, and hence a finite q_{el}, or not, for small departures from spherical symmetry, one cannot expect a proportionality between q_{latt} and q_{el}. The situation for large departures from spherical or cubic symmetry corresponding to large differences in c/a from ideal, as for Zn and Cd, will be discussed subsequently in this section.

An additional point that should be made about the results in Table 1 is that we have used the antishielding effect appropriate [55] for the conduction electrons that was discussed in Section 2.4. For Zn and Cd the γ_{eff}, or equivalently the induced EFG, δq^{ind}, from actual investigations by the procedure described in Section 2.4, was used. For Be^{2+} and Mg^{2+}, we have used the same value of 0.65 for the ratio $\gamma_{\text{eff}}/\gamma_\infty$ for the PW-PW contribution as was obtained [55] for Zn^{2+} and Cd^{2+}.

For Be metal the agreement between theory and experiment is seen from Table 1 to be not very good. However, this is not unexpected considering the fact that the total EFG involves a substantial cancellation between the lattice and electronic contributions. Additionally, there is also strong cancellation in the electronic contributions from different bands as we shall discuss in Sect. 2.6, where a comparison will be made between the results of APW and OPW calculations on this metal. Turning next to Mg, no experimental information is available for the sign of the EFG, but there is very good agreement between the magnitudes. If one assumes that the sign of the total EFG is indeed positive, as in theory, then the very good agreement between experimental and theoretical results provides indirect support for the lattice and electronic contributions and testifies, for the latter, to the accuracy of the electron density distribution obtained from the band calculations [58] by the OPW procedure. For Zn, the four experimental values [64–67] quoted for the EFG correspond to four different measurements of the coupling constant, two by Mössbauer effect [64, 65] and two by NQR spectroscopy [66, 67]. The agreement between the theoretical value [59] of the EFG and all four experimental values is quite satisfactory considering that the range of error in Q [74] of ^{67}Zn is about 10%. Finally for Cd, the agreement between experiment and theory is seen from Table 1 to be also quite satisfactory, of similar nature as for Zn. In the case of Cd, the experimental [68] value of the EFG, in contract to Be, Mg, and Zn metals, is not based on a Q derived from atomic data but rather from data on NQI in ionic crystals. In fact it is based [75] on the ratio between quadrupole coupling data for ^{113}In and ^{111}Cd* in the same ionic crystals. Since the In^{3+} ion is expected to cause stronger lattice distortion than the Cd^{2+} ion when acting as a substituent for a divalent ion in an ionic crystal, the error range in the value of Q of 0.77 barns for ^{111}Cd* is expected to be substantially larger than 10%, and perhaps larger than the 15% quoted in the literature [75]. In view of this, again, as for Zn, the agreement between theory [60] and experiment [68] for Cd metal is to be considered quite satisfactory.

Before terminating the discussion of the comparison between theory and experiment for the hexagonal close packed metals, we would like to emphasize again the role of antishielding effects on the electronic contribution to the field gradient. Thus if the antishielding factor [55] γ_{eff} of 0.65 γ_∞ had not been included in the electronic contributions eq_{el} to the EFG in Zn [59] and Cd [60], the eq_{el} for these two metals would have been considerably reduced, leading to net EFG's of 87.41 and 126.14 respectively in units of 10^{13} esu/cm^3, substantially smaller than the experimental values [68]. Another aspect of the role of γ_{eff} for the conduction electron contribution has to do with an empirical relation that has been proposed in the literature [56] from the analysis of a substantial amount of data from radiative methods, primarily PAC, on NQI's in pure metals and for impurity sites in non-cubic metals. This relation is

$$q_{\text{el}} = K\, q_{\text{ion}}^{\text{host}} (1 - \gamma_\infty)_{\text{impurity}}, \tag{35}$$

where $q_{\text{ion}}^{\text{host}}$ refers to the EFG at the nucleus at impurity site due to the ions in the host lattice, assuming no lattice distortion due to the presence of the impurity ion, γ_∞ is the antishielding factor for the impurity ion and K is an empirical factor that appears to lie between -2 and -3. The electronic contribution to the EFG can be derived from PAC data because these measurements determine the sign of the coupling constant and it is then possible to derive eq_{el} by substracting the lattice contribution to the EFG. The results in Table 1 for pure Zn and Cd give for K the values of -3.3 and -3.5 and therefore provide some support for the empirical relations in (35). More important, through the demonstration from ab initio investigations [55] for

γ_{eff}, that it is a sizeable fraction of γ_∞, one is able to get some physical support for a relation of the type in (35).

For the other two hcp metals, postponing the discussion of Be till the next section, one notices from Table 1 that for Mg, the empirical relation [56] in (35) does not hold at all, since K is expected to be positive because q_{latt} and q_{el} have the same sign. It appears then as if that the relation in (35) does not hold for small departures of c/a from the ideal hcp value and thus for small departures from cubic symmetry. A possible reason for this would be that for nearly cubic symmetry as has been found from ab initio investigation [57, 58] there are strong cancellations in the EFG contributions from various bands and various parts of $\boldsymbol{k}$-space. The net q_{el} therefore has a much too complicated origin to follow a simple relationship like that in (35). Further, it should be mentioned that for Mg^{2+} where $\gamma_\infty = -4.2$, if we had used γ_{eff} as less than $0.65\,\gamma_\infty$, the agreement between the theoretical and experimental values of the EFG would improve further beyond that in Table 1. It would thus be helpful to carry out ab initio calculations of γ_{eff} in Mg metal by a similar procedure as adopted [55] for Zn and Cd.

Again, in connection with this question of the effective antishielding factor γ_{eff}, we would like to mention that its incorporation has also been found to be very crucial for explaining (using [76] the hybridized OPW-TB procedure discussed in Sect. 2.3.4) the NQI for ^{129}Te measured [77] in the semiconducting phase of Te by ME. The NQI for the semi-metal Sb has also been investigated [78] by the tight-binding procedure leading to a successful explanation of the ^{121}Sb NQCC in this system as observed [79] by NQR. NQI data are also available [80] for Bi but no theoretical explanation has been attempted. It will be interesting to apply to this metal the TB procedure found to be very successful for Sb [78].

2.6. Comparison between field-gradients calculated by OPW and APW procedures – Application to Beryllium

To increase confidence in the calculated EFG's in metallic systems, in addition to comparison with experiment, it is desirable to compare the results by two different procedures for obtaining the band structure and electronic wave-functions. For a really critical test of the results by the two procedures, it is important not only to compare the total EFG's but also those from individual bands and for each band the EFG's for different $\boldsymbol{k}$ in the occupied regions of the Brillouin zone.

There is one such comparison available [43] in the literature, on Be metal. Both the energy bands and the field gradient as a function of $\boldsymbol{k}$ have been compared for the OPW and APW procedures. To test the sensitiveness of the results to the choice of potential, the APW calculations have been carried out for two different types of potential. The difference between the two potentials involves different choices for the exchange potential between the core and conduction electrons. For one of these potentials, the Slater statistical exchange approximation [39] was used while for the other, HF exchange [40] was used as in the case of OPW calculations.

As was expected, the OPW and APW results for the HF type exchange were found [43] closer to each other as compared to the APW results for the statistical exchange approximation. More details of the comparison are given in our paper [43] dealing with this work. We shall discuss here only the band by band comparison of the contributions to the EFG.

Table 2 presents the bandwise comparison of contributions to the EFG by the OPW and APW procedures using the same potential, namely the one for which HF exchange between core and conduction electrons was employed. As can be seen from this Table, the results for the first and second bands compare very well. For the third band, while the agreement is percentagewise not as good as for the first and second bands, there is still reasonable agreement, the OPW result being about 70 percent

Table 2. Conduction electron and lattice contributions to the electric field-gradient (in 10^{13} esu/cm^3) in beryllium by the APW and OPW procedures.

	APW	OPW
1st band	13.48	11.58
2nd band	−15.18	−14.80
3rd band	0.83	0.58
Sum	−0.87	−2.64
Ionic Sum	1.97	1.97
Total	1.10	−0.67
Experiment	± 1.40	

of the APW result. However, because of the strong cancellation between the sum of the first and third band contributions which is positive and the second band contribution which is negative, the net electronic contributions by the two procedures are in poor agreement. Both results have negative signs but the APW result is only about a third of the OPW result. The situation for the total EFG by the two procedures is worsened by further cancellation between the ionic and total electronic contributions, the total values having opposite signs for the two approaches. It would be quite useful to have an experimental determination of the sign of the EFG to decide which procedure provides better agreement with experiment. From the point of view of the magnitude of the EFG, there appears to be somewhat better agreement between the APW result and experiment. In principle, from purely theoretical considerations, one might expect the APW result to be somewhat more accurate for Be. The reason for this is that the Be^{2+} ion does not have any p-cores, so that there is no p-component built into the conduction electron wave function from the second, or orthogonality, term on the right in (5). The p-character of the conduction electron wave function near the nucleus, which makes the most important contribution to the EFG, is therefore determined completely by the summation in (4) over plane-waves with different $(\boldsymbol{k}+\boldsymbol{g}_i)$ vectors, which is not expected to converge rapidly. In the APW procedure, the p-character near the nucleus is determined by the atomic-like states inside the muffin-tin which are involved in (16) and the presence or absence of p-core electrons is not a crucial factor.

It would be interesting to carry out comparisons between the results by the two procedures for other metals, including the other hcp metals in Table 1. For Mg, there is a 2p core, so that one does not expect any convergence problems as in the case of Be. However, again, strong cancellations between individual bands are observed by the OPW procedure and it would be interesting to examine the nature of the agreement between the total EFG's by the two procedures as compared to the case of beryllium. For Zn and Cd, there are no severe cancellations between bands as in the cases of Be and Mg and one would expect much better agreement between the OPW and APW results. It would be interesting to see if this expectation is borne out by actual calculations.

2.7. Semimetals and semiconductors

We shall next remark briefly on the situation in semimetals and semiconductors which was touched on in Section 2.5.

Thus, in contrast to metallic systems for semiconductors (in the absence of any impurities which can donate electrons or holes), all the occupied bands are totally full [76, 81]. In semimetals, the highest occupied valence band and the next higher band may cross in some parts of the Brillouin zone, leading to pockets [82] of holes and electrons near the Fermi-surface. An example of a pure semiconductor where NQI data are available is Te [77], the technique involved being ME while Sb [79] and Bi [80] are two semimetals where NQR measurements have provided $e^2 q Q$.

Considering first the semi-metals, a theoretical investigation of the EFG has been carried out in Sb metal. For bands which are completely filled, one can write [78] the Bloch functions for the band electrons as

$$\psi_{\boldsymbol{k},n}(\boldsymbol{r}) = \sum_s e^{i\boldsymbol{k}\cdot r_s}\, \Phi_n(\boldsymbol{r}-\boldsymbol{r}_s)\,, \tag{36}$$

where $\Phi_n(\boldsymbol{r}-\boldsymbol{r}_s)$ represents the Wannier function [83] for the nth band centered around the sth lattice site. A good approximation to the Wannier functions is the orthogonalized atomic orbital function [78] obtained by orthogonalizing the atomic orbital associated with the energy level of the atom corresponding to the nth energy band to its neighbours. The electronic contribution to the EFG from the conduction electrons using the Bloch wave functions in (36) is given by

$$q_{\mathrm{el}} = \sum_s \int |\, \Phi_n(\boldsymbol{r}-\boldsymbol{r}_s)\,|^2 \left(\frac{3\cos^2\vartheta - 1}{r^3}\right) \mathrm{d}\tau\,. \tag{37}$$

Using this procedure, combined with small but significant corrections from the small pockets [82] at the boundary of the Brillouin zone associated with the conduction electrons and holes, good agreement has been obtained [78] with experiment [79].

For Te, both band calculations [76] involving basis functions which were hybrids [44] of OPW and TB functions, and MO calculations [84], using sizeable clusters of atoms to simulate the infinite solid, have provided satisfactory agreement with experiment [77]. The success of this latter calculation [84] for Te and the orthogonalized atomic orbital approach [78] to the Sb problem suggest that for semi-

conductor and semimetal calculations, cluster molecular orbital approaches [85, 86] would be quite satisfactory for explaining observed EFG's in these systems. This is an important observation since band investigations in impurity systems or semi-infinite systems such as surfaces are rather difficult. Impurity investigations by the cluster molecular orbital approach have already been carried out [85] for iodine and tellurium impurities in semi-conductors, providing satisfactory agreement with experimental NQI data from Mössbauer measurements. Similar investigations have been carried out [86] for adsorbed halogen atoms at semi-conductor surfaces and muonium in semiconductors. Cluster calculations are in progress [87] for indium metal surfaces to explain NQI data [88] from PAC measurements.

2.8. Temperature dependence of nuclear quadrupole interaction in metallic systems

Before concluding our discussion of the nuclear quadrupole interaction in pure metals, we would like to remark on the temperature dependence of the NQCC's. From experimental measurements, with the appropriate techniques, NMR [1] and NQR [2], ME [6], PAC [5] and other radiative methods, the EFG at the nuclei in metallic systems have been found to have the temperature dependence represented by [89]

$$q(T) = q(0)\,(1 - \beta T^{\alpha})\,. \tag{38}$$

The factor α appears to be close to 3/2 in most perfect metals and imperfect metallic systems, leading to what is referred in the literature [90] as $T^{3/2}$ law. However, there are a number of cases, especially at the nuclei of the impurities in some imperfect metallic systems, where there is significant departure [91] from this $T^{3/2}$ dependence.

For the understanding of the temperature dependence of the EFG, one has to consider the effects [92] of vibrational motions or phonons of the lattice on the various contributions to the EFG. Considering the fact that both the ionic charges on the lattice and the conduction electrons contribute to the EFG and that there can be three types of vibrational motions in the lattice as will just be explained, one expects [92] in general six types of phonon contributions to the temperature dependence. The three types of vibrational effects [93] can be characterized by harmonic, anharmonic, and anisotropic effects, arising from the corresponding natures of the effective potentials for the interaction between the ions. The harmonic effect refers to the normal harmonic oscillator type potential, proportional to the square of the ionic displacements, the anharmonic effect referring to cubic and higher power dependences and responsible for the expansion of the lattice with temperature. The anisotropic nature of the lattice vibrations refers to the variation in their amplitudes with direction, which would not be present in cubic lattices but would occur in lattices departing from cubic symmetry as in the cases of the metals with hexagonal close packed structures discussed in Section 2.5.

Some of these mechanisms have been treated parametrically [94] as well as from a more first principle [95] point of view in a number of metals. A comprehensive treatment [92] including all six mechanisms has been carried out for Zn and Cd. We shall only touch on some of the salient features of the results and conclusions from this latter work. Thus, it has been shown that as far as the lattice contribution to the EFG is concerned, the contribution from the isotropic lattice vibrations to the temperature dependence exactly vanishes [92]. The other five contributions to the temperature dependence are non-vanishing and their contributions are included in Figs. 2 and 3 for the two metals.

From Figs. 2 and 3, the major temperature dependence of the lattice contribution is seen to arise from the anharmonic lattice vibrations, this effect being evaluated by carrying out the lattice summation in (1) using the lattice parameters at different temperatures. The influence of the anisotropic lattice vibrations is smaller but significant and in the opposite direction. The temperature dependence of the electronic contribution derives its major contribution from the isotropic lattice vibrations. There are two ways that this temperature dependence arises [92], through the influence of the lattice vibrations on the potential experienced by the conduction electrons and the fluctuation they cause in the position of the nucleus at which the EFG due to the conduction electrons is being evaluated. These two effects manifest themselves through Debye-Waller factors [96] in the matrix elements of the potential and the structure factors in the expression for the EFG. The influence of anisotropic lattice vibrations on the EFG due to the conduction electrons was argued [92] to be rather small

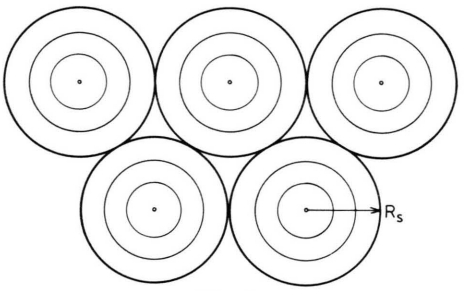

Fig. 1.

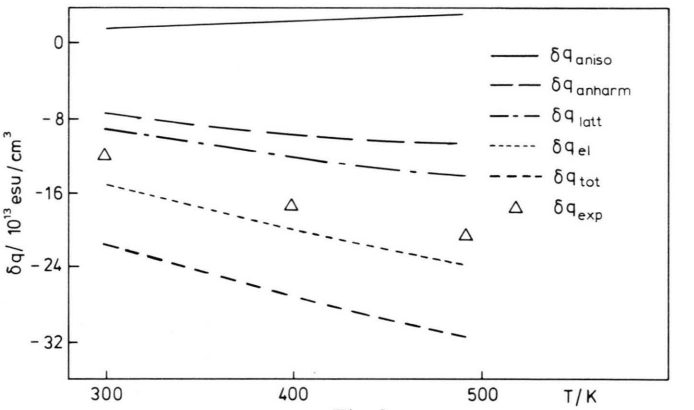

Fig. 2.

Fig. 1. Contour lines for the muffin-tin potential. R_s is the muffin-tin radius.

Fig. 2. Temperature dependence of the EFG in Zn. The calculated anharmonic and anisotropic lattice contributions are labeled δq_{anharm} and δq_{aniso} respectively, with δq_{latt}, δq_{el} and δq_{tot} being the net lattice, net electronic, and total changes in q, respectively. The experimental values δq_{exp} represented by Δ are obtained from [98].

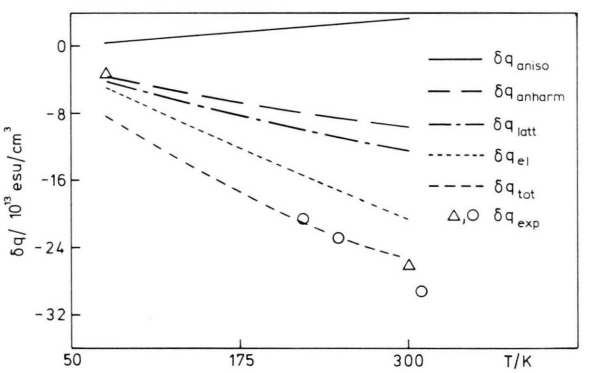

Fig. 3. Temperature variation of the EFG in Cd. The calculated anharmonic and anisotropic lattice contributions are labeled δq_{anharm} and δq_{aniso} respectively, with δq_{latt}, δq_{el} and δq_{tot} being the net lattice, net electronic, and total changes in q, respectively. Δ represents data obtained from *R.* S. Raghavan and P. Raghavan in Ref. [97], and 0 represents data obtained from J. Bleck et al. also from [97].

compared to that of the isotropic lattice vibrations and was not included. The influence of the anharmonicity of the lattice vibrations was studied as in the case of the lattice contribution by evaluating the electronic contribution for the different lattice constants at different temperatures. It was found [92] to contribute less than 5% of the temperature dependence arising from the influence of the isotropic component of the lattice vibrations. Because of its smallness, the anharmonicity contribution is not shown separately but is combined with the isotropic contribution, the combined contribution being represented as δq_{el} in the Figs. 2 and 3. From the Figs. 2 and 3, the electronic contribution to the temperature variation of the EFG is seen to be substantially larger than the lattice contribution although both have the same sign. The comparison between the net theoretical changes in the EFG's with temperature and experiment for the two metals indicates that for Cd, there is good agreement between theory [92] and experiment [97] in the range $200 \leqq T/\text{K} \leqq 300$ where most of the experimental data is available. There is one experimental point available at liquid nitrogen temperature which indicates a significantly weaker temperature variation than predicted by theory. More experimental points are needed in this temperature region to clarify the situation. For Zn, the experimental [98] variation in the EFG with temperature to be about a factor of two weaker than predicted by theory. It would be interesting to test if the theoretical temperature dependence for the net EFG is significantly influenced in the two metals by the use of more accurate phonon distribution curves from theory or experiment than from the Debye model used [92] for evaluating the Debye-Waller factors [96]. It would also be interesting to study the temperature dependence of the electronic contribution by other procedures, such as the APW procedure besides the OPW procedure based on pseudopotential theory used in the work on Zn and Cd. Such analysis would throw some light on the factors

that could bridge the remaining difference between theory and experiment for Zn. However, overall, there appears to be reasonably satisfactory agreement [92] between the theoretical and experimental temperature dependences for Zn and Cd. Since the experimental temperature dependences [97, 98] for these two metals appear to follow the $T^{3/2}$ law [90] it appears that theory supports this law. However, in view of the different temperature dependences predicted by the various different mechanisms as seen from the Figs. 2 and 3, one cannot generalize that a $T^{3/2}$ behaviour will be expected in general from theory. Instead, what the theoretial analysis shows is that all mechanisms contributing to the temperature dependences of the EFG have to be carefully evaluated and combined in making comparisons with experiment.

In concluding this discussion of the EFG's in pure metals, it should be mentioned that there have not been as comprehensive theoretical investigations of the pressure dependence [99, 100] of the EFG as for the temperature dependence. A substantial contribution to the pressure dependence is of course expected from changes in lattice parameters with pressure. However the important dependence [92] of the EFG on isotropic and anisotropic lattice vibrations (or phonon effects) discussed in this Section suggests that the influence of pressure on the phonon spectrum and consequently on the electronic and lattice contributions to the EFG will have to be incorporated in attempting a quantitative comparison between theoretical and experimental temperature dependences.

3. Origin of Nuclear Quadruple Interaction in Imperfect Metallic Systems

NQI data are available in metallic systems with various kinds of point defects among them, substitutional impurities as in dilute alloys [101–107], interstitial impurities such as muons in metals [108, 109] and vacancies [102, 110]. Such data are obtained for the host atom nuclei adjacent to the imperfection from both conventional NMR [111] as well as special double resonance techniques [112] and muon spin rotation technique [108, 109]. For the solute nuclei, the main source [104] of data is from $\gamma-\gamma$ or $\beta-\gamma$ PAC [3] as well as related techniques [4, 5] and from ME [6].

The general equation (1) in Section 2 of course holds for these imperfect systems. The main problem in making use of it is the difficulty in the determination of the electron density $\varrho(\boldsymbol{r})$ and positions of the ions in the presence of the imperfection. Unlike the case of pure metals, the positions of the ions in the lattice adjacent to the imperfection are not readily measurable, although some information can be obtainable from EXAFS measurements [113]. Secondly the lack of short range periodicity makes the determination of the electronic wave-functions, and hence the charge density, difficult.

In Sects. 3.1 and 3.3 we shall briefly discuss the mechanisms that can contribute to the perturbation in $\varrho(\boldsymbol{r})$, from that in the perfect host lattice, in the presence of the impurity as well as lattice distortion effects and the expected influence of these effects on EFG's at the host and impurity nuclei. In Sects. 3.2 and 3.4 we shall consider two sets of systems that we have worked on, as illustrations of the contributions to the EFG's from some of these factors. This will allow an assessment of the current procedures for analyzing the origins of EFG's in imperfect systems and to reach conclusions about possible directions to improve the understanding of this rather complex field.

3.1. Discussion of sources contributing to the electric field-gradients at host nuclei in the presence of imperfections

Considering first a cubic metal host, the EFG's at the nuclei in the perfect metal vanish due to the cubic symmetry of the environment about them. When a point imperfection or impurity (we shall use the two terms interchangeably) is introduced, such as a solute atom in a dilute alloy, a vacancy, or a positive muon in an interstitital position to be discussed in the next section, the cubic symmetry of the environment can break down due to two reasons. If the impurity carries a formal charge Z' (such as in the case of a zinc impurity in a copper lattice, the divalent Zn^{2+} ion carrying a formal charge of unity, or a vacancy in a copper lattice, which would be considered to carry a negative formal charge, or the positive formal charge for the muon in the interstitial position) then the extra potential due to the formal charge can produce a perturbation [114–124] in the conduction electron density in its surroundings, leading to a breakdown

of cubic symmetry at the neighbouring host nuclei and hence to a finite EFG. A change in conduction electron density can be brought about also by a solute ion which does not carry a formal charge. This can happen in two ways: a) The difference in the ionic potential (from the nuclear charge and electrons on the ion) between the solute ion and the host ion it replaces can act as a source of perturbation, b) Lattice distortion can occur due to the difference in the sizes of host and solute ions, involving displacements of host ions neighbouring the solute ion, which in turn can lead to a change in the potential experienced by the conduction electrons. The lattice distortion [123, 125–129] of course, in addition to its indirect effect through the change in the conduction electron distribution it produces, is also a direct source of EFG's at the host nuclei. This is because the lattice distortion destroys the cubic arrangement of neighbouring ions around the host nuclei which can lead to a finite EFG from the charges on these ions. The lattice distortion can arise not only due to the difference in sizes of the host and solute ions but also their difference in charges, the accompanying change in conduction electron distribution leading to changes in the potentials at the ion sites and hence a redistribution in their positions. Thus, there are a number of causes associated with the distortions in the electron distribution and lattice positions, and their interactions, which can lead to a local departure from cubic symmetry around the host nuclei and the appearance of EFG's.

It is because of this complexity of the whole problem that the electronic and lattice contributions to the EFG's in these systems have been treated in approximate ways so far. We shall now briefly discuss these mechanisms starting with the electronic contribution first. It should be pointed out that in non-cubic metals, these electronic and lattice contributions brought about by the presence of the impurity will also lead to changes in the EFG's at host ion nuclei in the perfect host metal, the EFG's being of course finite even in the absence of the impurity. There have not been many studies of EFG's at host nuclei in non-cubic metals, the major studies in these systems having been carried out at the impurity sites using nuclear radiative techniques. We shall consider this latter situation in Sects. 3.3 and 3.4. Our discussions in the rest of this section and the next will be confined to host ion nuclei in cubic hosts containing imperfections.

The earliest theoretical treatment of the conduction electron contribution to the EFG (also referred to in the literature as valence contribution) at host nuclei in cubic host metals was carried out simultaneously by Kohn and Vosko [115] and Blandin and Friedel [116]. These authors considered the scattering of the Bloch electrons due to the perturbing potential produced by an impurity with a formal charge Z'. In the asymptotic region, at large distance from the impurity, the scattered wave solution can be written in the form

$$\Phi_{\boldsymbol{k}}(\boldsymbol{r}) = \psi_{\boldsymbol{k}}(\boldsymbol{r}) + \frac{f(\boldsymbol{k}, \boldsymbol{k}')}{r} \psi_{\boldsymbol{k}}(\boldsymbol{r}) , \tag{38}$$

where $\boldsymbol{k}$ is the crystal momentum for the Bloch electron with wavefunction $\psi_{\boldsymbol{k}}(\boldsymbol{r})$ in the perfect host and $\boldsymbol{k}'$ has the same magnitude as $\boldsymbol{k}$ but a direction corresponding to $\boldsymbol{r}$, the radius vector joining the impurity and the host nucleus whose EFG is of interest. It is assumed that the function $f(\boldsymbol{k}, \boldsymbol{k}')$ depends only on the magnitude of $\boldsymbol{k}$ and the angle θ between $\boldsymbol{k}$ and $\boldsymbol{k}'$, so that one can write it as $f_k(\theta)$. As is usual in scattering theory, one can expand $f_k(\theta)$ in terms of phase shifts η_l in the form

$$f_k(\theta) = \frac{1}{2ik} \sum_{l=0}^{\infty} (2l+1)\,(e^{2i\eta_l(k)} - 1)\, P_l(\cos\theta) , \tag{39}$$

$P_l(\cos\theta)$ being the Legendre polynomial. Equation (38) for the perturbed function $\Phi_{\boldsymbol{k}}(\boldsymbol{r})$ is used to derive [115, 116] the net change in electron density $\delta\varrho(\boldsymbol{r})$ at any point described by radius vector $\boldsymbol{r}$ with respect to the impurity, a summation being carried out over all occupied $\boldsymbol{k}$ states lying below the Fermi surface. Assuming the Fermi surface to be spherical, the expression for $\delta\varrho(\boldsymbol{r})$ is given by

$$\delta\varrho(\boldsymbol{r}) = -\left(\frac{1}{4\pi^2}\right)\left(\frac{1}{r^3}\right) \cdot \left\{\exp(2ik_F r)\,[u_{\boldsymbol{k}_F}(\boldsymbol{r})]^2\, k_F f_{k_F}(\pi) + \begin{matrix}\text{complex}\\ \text{conjugate}\end{matrix}\right\} , \tag{40}$$

where $\boldsymbol{k}_F$ is in the direction of $\boldsymbol{r}$ and $u_{\boldsymbol{k}}(\boldsymbol{r})$ are the periodic functions in the Bloch wave-functions for the host metal:

$$\psi_{\boldsymbol{k}}(\boldsymbol{r}) = e^{i\boldsymbol{k}\cdot\boldsymbol{r}} u_{\boldsymbol{k}}(\boldsymbol{r}) . \tag{41}$$

On substituting $u_{\boldsymbol{k}_F}(\boldsymbol{r}) \equiv 1$, the expression for $\delta\varrho(\boldsymbol{r})$ in (40) reduces to the corresponding form for free

electrons scattered by the impurity that has been derived by Friedel [114], namely

$$\delta\varrho_{\text{free}}(\boldsymbol{r}) = A\cos(2k_{\text{F}}r+\varphi)/r^3\,, \tag{42}$$

where the quantities A and φ are related to the phase shifts η_l. Using the expression for $\delta\varrho(\boldsymbol{r})$ in (40) the EFG (at a host nuclear site described by the radius vector $\boldsymbol{r}_s$ with the impurity as origin) due to the combined effect of the formal charge Z' on the impurity and the electron density change $\delta\varrho(\boldsymbol{r}_s)$ produced by it at a host nuclear site $\boldsymbol{r}_s$ has been derived [115, 116] to have the form

$$q^{\text{v}} = \frac{8\pi}{3}\,\alpha(\boldsymbol{k}_{\text{F}})\,\delta\varrho_{\text{free}}(\boldsymbol{r}_s)\,, \tag{43}$$

where q^{v} represents the maximum component of the valence contribution to the EFG tensor in the direction of $\boldsymbol{r}_s$, about which $\overleftrightarrow{q}^{\text{v}}$ is axially symmetric, and

$$\alpha(\boldsymbol{k}_{\text{F}}) = \frac{\int[\psi_{\boldsymbol{k}_{\text{F}}}(\boldsymbol{r})]^2\,P_2(\cos\theta')\,r'^{-3}\,\mathrm{d}\tau'}{\int e^{2i\boldsymbol{k}_{\text{F}}\cdot\boldsymbol{r}'}\,P_2(\cos\theta')\,r'^{-3}\,\mathrm{d}\tau'} \tag{44}$$

is the enhancement factor due to the fact that the conduction electrons are represented by Bloch wavefunctions and not plane waves. For the latter, $\alpha(\boldsymbol{k}_{\text{F}})$ would be equal to unity. In (44), $\boldsymbol{k}_{\text{F}}$ represents the Fermi momentum vector in the direction of $\boldsymbol{r}_s$ and θ' the angle between the integration vector $\boldsymbol{r}'$ and $\boldsymbol{r}_s$. In deriving (43), two assumptions have been made. One is that the contribution to the EFG from the formal charge Z' on the impurity is almost completely cancelled [116] by the effect of the density fluctuation $\delta\varrho(\boldsymbol{r})$ long before one reaches the neighbourhood of the host nucleus of interest and that the EFG at the host nucleus arises from $\delta\varrho(\boldsymbol{r})$ in the vicinity of this nucleus. The other assumption is that antishielding effects due to the cores of the host ion containing the nucleus of interest may be neglected. The first assumption is a reasonable one for host nuclei far away from the impurity but needs to be corrected, as will be discussed later in this Section, for nuclei at nearest neighbour sites as well as others not too far away such as the second and third nearest neighbours. The influence of antishielding effects on $\alpha(\boldsymbol{k}_{\text{F}})$ can be incorporated [115] using the antishielding function $\gamma(r')$ discussed in Sect. 1 and 2.4 leading to

$$\alpha(\boldsymbol{k}_{\text{F}}) = \frac{3}{8\pi}\int e^{2i\boldsymbol{k}_{\text{F}}\cdot\boldsymbol{r}'}[u_{\boldsymbol{k}_{\text{F}}}(\boldsymbol{r}')]^2 \cdot \frac{P_2(\cos\theta')}{r'^3}\,(1+\gamma(r'))\,\mathrm{d}\tau'\,. \tag{45}$$

The factor $3/8\pi$ arises out of the fact that the integral in the denominator in (44) involving plane waves has a magnitude of $8\pi/3$.

In using (43), combined with $\alpha(\boldsymbol{k}_{\text{F}})$ in (45), for evaluating q^{v}, one needs a knowledge of A and φ. Since these two quantities are related to the phase shifts η_l for scattering of free electrons, one could use the first Born approximation [130] to derive these phase shifts. This would lead to two difficulties. First, one would need an explicit form for the impurity potential and secondly it would be equivalent to handling this potential in first-order perturbation theory, presupposing the impurity potential to be weak. Instead, in the literature [114, 115] A and φ have been derived by retaining the contributions to them from only the s and p phase shifts. These phase shifts have been derived from two equations, corresponding to the Friedel sum rule [114–116]

$$Z' = \frac{2}{\pi}\sum_{l=0}^{\infty}(2l+1)\,\eta_l(k_{\text{F}})\,, \tag{46}$$

Z' being the formal charge on the impurity, and another equation [115, 116] relating the residual resistance of the dilute alloy to the $\eta_l(k_{\text{F}})$. Only the s and p phase shifts are retained in the summation in (46) and that in the expression [115] for the residual resistance.

NQI data are now available at host nuclear sites [102, 103, 108–110] close to the impurity, including the nearest neighbours in both substitutional and interstitial systems. The approximation of a large distance between host nucleus and impurity used in deriving (45) for q^{v} would not be valid for these situations and corrections are needed in two respects. The first is that the assumption [115, 116] that the EFG due to the formal charge on the impurity is totally neutralized by the density fluctuation $\delta\varrho(\boldsymbol{r})$ in the region between the immediate vicinity of the nucleus and the impurity is no longer valid. Secondly, one has to make use of an expression for the density fluctuation $\delta\varrho(\boldsymbol{r})$ that is valid for shorter distances from the impurity than the asymptotic region. Efforts to correct for the effects of these two approximations have been made by a number of investigators [117–121, 123, 124, 129]. We shall summarize here some of the approaches that have been used for the study of $\delta\varrho(\boldsymbol{r})$ and EFG's in the preasymptotic region. The reader is reforced to the individual papers in the literature

[117–121, 123, 124, 129] for details and further discussions.

Regarding the influence of incomplete cancellation of the EFG due to the impurity charge, the following expression has been utilized [123, 124, 129, 131–133]

$$q^{\nu} = \frac{8\pi}{3}\alpha(\boldsymbol{k}_F)\left[\delta\varrho_{\text{free}}(\boldsymbol{r}) + \frac{3}{4\pi r^3}\cdot\int_r^\infty\int_0^\pi\int_0^{2\pi}\delta\varrho(\boldsymbol{r}')\,r'^2\,dr'\,d\cos\theta'\,d\Phi'\right]. \tag{47}$$

For the asymptotic region, r is large and the second term in the square brackets in (47) reduces to zero, so that (47) reduces to the form in (43).

The second correction involves replacing $\delta\varrho_{\text{free}}(\boldsymbol{r})$ in (43) by an expression for the density fluctuation that holds in the preasymptotic region. One of the procedures for this is to replace the expression (42) for $\delta\varrho_{\text{free}}(\boldsymbol{r})$ by a summation of the form [117]

$$\delta\varrho_{\text{free}}(r) = \sum_{n=1}^{\infty}\frac{A_n\cos(2k_F r + \Phi_n)}{r^{2+n}} \tag{48}$$

with the parameters A_n and Φ_n involving first and higher derivatives of the phase shifts $\eta_l(k)$ with respect to k for the Fermi wave-vektor $\boldsymbol{k}_F$. Applications [128, 129, 131, 132] have been made of this expression including up to the second term, $n = 2$.

The evaluation of $\delta\varrho_{\text{free}}(r)$ for the preasymptotic region has also been attempted [119] using a perturbation approach involving the difference in pseudopotentials of the impurity and host atoms. Self-consistency effects have been incorporated [119] using a dielectric shielding function [134] including exchange effects. The $\delta\varrho_{\text{free}}(r)$ derived in this way shows oscillatory behaviour with respect to the impurity, the behaviour in the asymptotic region being similar that given by (42). The pseudopotential approach has been criticized [135] on the basis that the difference in impurity and host potentials may be too strong to handle within the framework of first-order perturbation theory and that the results depend rather sensitively on the choice of the pseudopotential.

Another approach [120–123, 135] that can be described as a self-consistent non-linear response theory involves the solution of the Schrödinger equation for the system with the impurity at the center. The potential in the Schrödinger equation was determined by the nuclear charge of the impurity atom, the Coulomb and exchange potentials associated with the electrons in the system (exchange being included within the framework of the statistical exchange approximation [39]), and the potential due to a uniform positive background with average density determined by the nuclear charges of the host nuclei. This latter approximation is referred to in the literature as the jellium approach. $\delta\varrho(\boldsymbol{r})$ due to the impurity has been obtained in this approach by carrying out the calculations first with the impurity ion at the substitutional site and then the host ion and taking the difference in the densities $\varrho_I(r)$ and $\varrho_H(r)$. For an interstitial impurity [121] only $\varrho_I(r)$ with the impurity at the interstitial site, is necessary. As an improvement on this procedure, the jellium approximation for the background potential from the ion in the lattice has been replaced [136] by a spherical solid approximation [120, 136, 137], where the charges of the ions in the lattice are replaced by their spherical average. These two approaches, the jellium and spherical solid models, of course have the limitations that the influence of the potential due to the ions in the host lattice, which would be in discrete periodic positions in the perfect lattice, is being approximated by the homogeneous jellium or isotropic spherical solid models and furthermore, the statistical approximation to the exchange interaction is used, which limits the accuray of magnetic and nuclear quadrupole hyperfine properties [138, 139]. However, the non linear response procedures [120–123, 135] have the merits of avoiding the perturbation approximation, which is not appropriate when the impurity potential is relatively strong, and also of incorporating self-consistency within the framework of the models employed.

The dependences of $\delta\varrho(r)$ on r for a vacancy in aluminium from a recent calculation [136] using both the jellium and spherical solid approximations are shown in Figure 4. The results with the two approximations agree well at large r but differ significantly for small r. This suggests that the introduction of the actual lattice potential, which will lead to greater inhomogeneity than with the spherical solid approximation, would probably result in further significant changes in $\delta\varrho(r)$ at smaller r.

Lattice distortion effects associated with the presence of substitutional and interstitial impurities and vacancies and their effects on the EFG have been

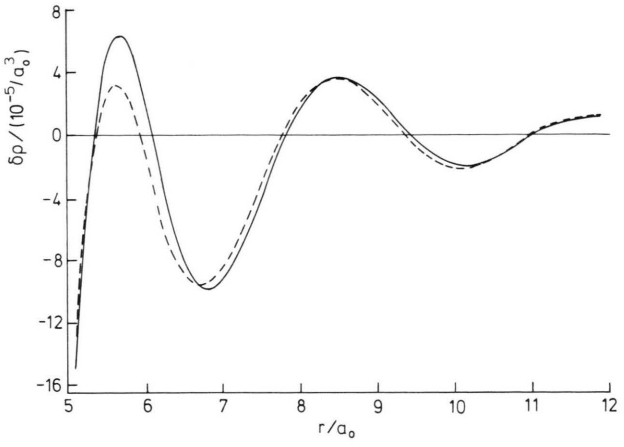

Fig. 4. Variation of the perturbation $\varrho(r)$ in electron density with distance r from a vacancy in Al (Ref. [136]), using the self-consistent non-linear response procedure. The dashed and continuous lines refer to the jellium and spherical solid approximations respectively. a_0 is the Bohr radius.

treated [123–125, 127, 129, 131, 132, 135, 136, 140] so far primarily in terms of continuum elastic distortion approaches [129, 140]. There has been one attempt [128] to take account for the discreteness of the lattice which shall be discussed after describing the continuum approaches that have been employed.

The version of the continuum model [129] that has been used most extensively, assumes radial displacements of the host ions about the impurity of the form

$$\boldsymbol{u} = D\,\frac{\boldsymbol{r}}{r^3} \tag{49}$$

with D given by the relation

$$D = \Delta V/4\pi\gamma_E\,, \tag{50}$$

ΔV being the change in volume of the lattice per impurity using the misfitting sphere model [141] for the impurity. The misfit arises for instance from the difference in impurity and host ion radii for substitutional impurities or from the impurity ion being inserted in an interstitial region which was previously empty.

γ_E is related [141] to the Poisson ratio σ for the host material by

$$\gamma_E = \frac{3(1-\sigma)}{1+\sigma}\,, \tag{51}$$

being about 1.5 for most metals. The volume parameter ΔV is obtained from the relation [141]

$$\Delta V = \frac{3}{4}\,a^2\,\frac{\mathrm{d}a}{\mathrm{d}c}\,, \tag{52}$$

where a is the lattice parameter for the host lattice and $\mathrm{d}a/\mathrm{d}c$ its rate of change with respect to impurity concentration.

One could obtain the contribution to the EFG from ionic charges by carrying out lattice summations of the form given by the first term in (1) using lattice positions in the cubic distorted lattice obtained by including displacements given by (49). This contribution, referred to as the direct size effect or simply size effect in the literature, has instead usually been obtained in a semi-empirical manner as follows [129]. Thus, from symmetry arguments, one can relate [125] the components of the EFG tensor at any point described by position vector $\boldsymbol{r}_s$ with respect to the impurity as origin to the strain components ε_{ij} produced by the lattice distortion through the equation

$$\begin{aligned} q^s_{ij} &= \frac{1}{e}\,(V_{ij} - \tfrac{1}{3}\nabla^2 V) \\ &= \frac{1}{e}\,[(F_{11}-F_{12})\,\delta_{ij}\,(\varepsilon_{ii} - \tfrac{1}{3}\sum_k \varepsilon_{kk}) \\ &\quad + 2(1-\delta_{ij})\,F_{44}\,\varepsilon_{ij}]\,, \end{aligned} \tag{53}$$

where

$$\varepsilon_{ij} = \frac{1}{2}\left(\frac{\partial u_i}{\partial x_j} + \frac{\partial u_j}{\partial x_i}\right) \tag{54}$$

with i, j, and k referring to x, y, and z and the F_{mn} referring to the components of a fourth order tensor. The components of the tensor F_{mn}, or rather the combination $(F_{11}-F_{12})$ and F_{44} which occur in (53), have been obtained in the literature in the following manner [129]. Thus, assuming a uniform strain in a fcc lattice and carrying out the summations over unit charges over the twelve nearest neighbours leads to [126]

$$F_{11} - F_{12} = -3\,F_{44} = 18\sqrt{2}\,e/a^3\,, \tag{55}$$

where a is the lattice parameter. This expression has been utilized [129] with an empirical factor λ, the argument give for this factor being that the result [126] in (55) is based on unshielded point charges. The factor λ could in principle incorporate antishielding effects due to core electrons. It could also include in an indirect manner the influence of the response of the conduction electrons to the change in potential produced by the movement of the host ions from their original positions due to lattice distortion and a correction for the fact that (55) involved only the summation over the first twelve

neighbours in the fcc lattice. The actual expression used for $(F_{11} - F_{12})$ and F_{44} is thus given by [129]

$$F_{11} - F_{12} = -3F_{44} = \frac{18\sqrt{2}\,\lambda e}{a^3}. \tag{56}$$

As an illustration of the combined use of (49) through (54) and (56), the expressions for the EFG tensor components at the first nearest neighbour of an impurity in a fcc lattice would be given by [129]

$$q^{s}_{xx} = \frac{54\sqrt{2}\,\lambda}{16\pi\gamma_E}\left(\frac{1}{c}\frac{da}{dc}\right)\frac{d_1^3}{a},$$

$$q^{s}_{yy} = q^{s}_{zz} = -\frac{27\sqrt{2}\,\lambda}{16\pi\gamma_E}\left(\frac{1}{c}\frac{da}{dc}\right)\frac{d_1^3}{a}, \tag{57}$$

$$q^{s}_{yz} = \frac{27\sqrt{2}\,\lambda}{16\pi\gamma_E}\left(\frac{1}{c}\frac{da}{dc}\right)\frac{d_1^3}{a},$$

where $d_1 = a/\sqrt{2}$ is the nearest neighbour distance. The presence of the off-diagonal term in (57) leads to the results that the principal axes for the size-effect contribution to the EFG tensor do not coincide with the crystal axes, and furthermore, that the EFG tensor is not axially symmetric about the line joining the impurity and the host nuclear site under question, in contrast to the axial symmetry expected for the valence contribution. This feature of the possibility of having a finite asymmetry parameter due to the size-effect tensor q^s is a result of the occurrence of the fourth rank tensor F_{mn} in (53) which brings in the local symmetry of the host lattice point in the crystal. Of course, to get the principal component of the net $\vec{q}$, one has to add the components q^{v}_{ij} and q^{s}_{ij} and diagonalize the sum. The EFG tensor at the second nearest neighbour site is expected from these considerations to be axially symmetric.

The expression for q^{s}_{ij} in (53) has been used for the first through fourth nearest neighbours in several alloys with copper as host [124] for Mg-Al alloy [131] and vacancy in aluminium [132]. For the copper alloy work, using different λ for different neighbours, values ranging rather widely from $\lambda = -25$ to $\lambda = +87$ have been obtained in attempting to get agreement with experimental data. For the aluminium work [131, 132] one value of λ has been used for all neighbours, the value being obtained by fitting theory and experiment for one set of neighbours, the values of λ needed being -18 for the alloy [131] and -85 for the vacancy [132], again a wide variation.

An alternate form of the displacement vector $\boldsymbol{u}$ has been proposed [135, 140] in the literature, namely

$$\boldsymbol{u} = A\frac{\boldsymbol{r}}{r^3}\cos(2k_F r + \Phi). \tag{58}$$

While there is no rigorous reason for choosing this form, this form has been suggested as a plausible one because the perturbed electron density in (42) shows such an oscillatory behaviour. Some other arguments have also been cited [140] in support of this form for the displacement vector. The phase factor Φ is obtained from elastic theory [142] and the parameter A is determined [136, 140] by fitting to the results of ab initio calculations [143–145] of lattice displacement where available, thus indirectly bringing in some features of the discreteness of the lattice into the theory. The rest of the procedure [135] in relating this expression for the displacement vector to the EFG components is the same as before, utilizing for this purpose (53), (54) and (56). The parameter λ is again determined [135, 136] by fitting the experimental NQI data for one set of neighbouring host nuclei to the theoretical results obtained by summing the valence and size effect contributions. Applications [135, 136, 140] have been made to systems involving vacancies in Al and Cu and a number of substitutional Al alloy systems. The values of λ needed in this procedure are considerably smaller, in the region -1 to -5. The size effects for ^{63}Cu and ^{27}Al nuclei which are nearest neighbours to a positive muon in the corresponding metals have been evaluated [136] by this procedure using the oscillatory displacement vector. We shall discuss the results in the next section, where we combine them with the valence contributions obtained using the values of $\alpha(\boldsymbol{k}_F)$ that we have derived [146] for these metals and compare with experimental results from μSR measurements [108, 109].

Finally, as has been mentioned earlier, a discrete summation of the contributions to the EFG from the displaced ions in the lattice using the expression in the first term in (1) has been carried out [128] for a vacancy in Al. The displaced ion positions of the ions used in this work were taken from ab initio investigations [143]. This obviates the need for using the fourth rank tensor F_{mn} in the elastic continuum

approximation and hence of the empirical parameter λ. The use of this procedure would of course be limited to those imperfect systems in which results of time-consuming ab initio investigations of host ion positions are available.

Lastly, we would like to remark on the question of the influence of lattice distortion on the perturbation of the electron density and vice versa. There are two effects discussed [129] in the literature concerning the former. The first is that one should use the electron density fluctuation $\delta\varrho(\boldsymbol{r})$ of the displaced host ion position in (47) rather than the undisplaced position in the perfect host. One would not normally expect any significant effect due to this modification, especially for the distant host nuclei, since even at the nearest neighbours of the impurity, the fractional displacements [143–145] are 3% or less. The second effect mentioned [129] in the literature is a correction to the Friedel sum rule in (46) involving the summation over scattering phase shifts η_l. This rule has been modified and the following replacement Z'_{eff} has been proposed [147] for the formal charge Z' in (46), namely

$$Z'_{\text{eff}} = \left(1 - \frac{3}{\gamma_E}\frac{1}{a}\frac{\mathrm{d}a}{\mathrm{d}c}\right) Z' . \tag{59}$$

In the treatments of the valence contributions to the EFG's at host nuclei based on the asymptotic form (42) or the preasymptotic form (48), the influence of this correction is taken care of by using the Hurd-Gordon phase-shifts [148] for the evaluation of A and Φ (or A_n and Φ_n in (48)) which take account of the Blatt correction in (59) to the phase shifts. The Blatt correction has also been incorporated [135] into other procedures for $\delta\varrho(\boldsymbol{r})$ including the nonlinear response procedure [120–123] discussed earlier.

As regards the influence of the electron density perturbation on the lattice distortion effect, the use of the adjustable parameter λ in both the elastic continuum procedures used in the literature can in principle include part of this effect indirectly because it is determined by matching theoretical and experimental EFG's for certain neighbouring host ion nuclei. Also the use of the relation (50) for the parameter D in the host ion displacement vectors (Eq. (49)) would indirectly include part of the influence of the electronic density perturbation because the latter can affect the change in lattice parameter due to the presence of the impurity and hence $\mathrm{d}a/\mathrm{d}c$ (Equation (57)).

3.2. Electric field-gradient at nearest neighbour site in copper and aluminium due to muonium at interstitial site

The presence of a μ^+ ion at an interstitial site in a cubic metal destroys the cubic symmetry at the nuclear sites at the neighbouring nuclei leading to finite EFG's at these sites. The finite NQI at the nearest neighbour nuclear sites due to these EFG's have been obtained [108, 109] from the magnetic field-dependence of the line-widths of muon spin rotation spectra [149]. The muon spin rotation (μSR) spectrum is related to the Larmor precession effects for μ^+ in applied or internal fields in course of its decay into a positron, neutrino and antineutrino. The process of extraction of this NQI is well described [149]. We shall be concerned here with only the origin of the observed NQI's at the neighbouring nuclei.

From the NQCC's obtained from μSR measurements [108, 109] for the nearest neighbour ^{63}Cu and ^{27}Al nuclei in Cu and Al, the EFG's at these sites have been derived to be $13.0 \cdot 10^{+13}$ esu/cm^3 and about $8.6 \cdot 10^{+13}$ esu/cm^3 respectively. We have analyzed the valence contribution to the EFG using (45) and (47). The enhancement factor $\alpha(\boldsymbol{k}_F)$ defined in (45) (with $\boldsymbol{k}_F$ representing the Fermi momentum in the direction joining the impurity and the nucleus at which the EFG is being studied) has been calculated [146] using band wave-functions for the two metals by both APW and OPW procedures. The values obtained for $\alpha(\boldsymbol{k}_F)$ are not only of interest because they represent the first ab initio investigations of this factor using both accurate band wave-functions for the pure metal and antishielding effects, but also because they represent the first comparison for α by two independent methods using the same potential and by the same group. We shall briefly describe our procedures and results for $\alpha(\boldsymbol{k}_F)$ and then proceed to the comparison between our calculated valence contributions and experimental results.

The $\alpha(\boldsymbol{k}_F)$ in our work were evaluated using (45). The direction of the Fermi momentum corresponds to the $\langle 100 \rangle$ direction. For Cu, for both the APW and OPW functions, a potential used in the literature for earlier calculations [150] of the band-structure and Fermi surface dimensions has been utilized. For Al, we have utilized a potential used in earlier OPW calculations [151] for analysis of the Fermi

surface and Knight shifts in NMR measurements. For the incorporation of antishielding effects, one can utilize for both the OPW and APW investigations the procedure [55] described in Section 2.4.

The convergence of $\alpha(\boldsymbol{k}_F)$ with the sizes of the basis sets was tested carefully [146] for both the OPW and APW investigations and it was found that for the OPW case with 52 basis functions, a convergence of about one percent was attainable for Cu and about 3 percent for Al. For the APW case, the rate of convergence was comparable to OPW for Cu but was substantially faster for Al.

The results for $\alpha(\boldsymbol{k}_F)$ found by these procedures are:

$$\alpha(\boldsymbol{k}_F)_{\text{Al-OPW}} = 13.7; \qquad \alpha(\boldsymbol{k}_F)_{\text{Al-APW}} = 10.1; \tag{60}$$

$$\alpha(\boldsymbol{k}_F)_{\text{Cu-OPW}} = 36.3; \qquad \alpha(\boldsymbol{k}_F)_{\text{Cu-APW}} = 29.5. \tag{61}$$

It is gratifying that the values of α by the OPW and APW procedures compare well for both metals, complementing the satisfactory agreement found [43] by the two procedures for band by band results for the EFG in pure Be discussed in Section 2.5.

Before discussing the results obtained for the valence contributions to the EFG's at ^{63}Cu and ^{27}Al nuclei at the nearest neighbour sites of muon using (47) and our calculated $\alpha(\boldsymbol{k}_F)$, we would like to compare the latter with results from earlier investigations. Thus, for Al, there have been a number of earlier investigations of $\alpha(\boldsymbol{k}_F)$. Among these, there was one [152] in which the Bloch wave-functions for the conduction electrons were taken as linear combinations of OPW wave-functions. But instead of obtaining them by a variational method as in Sect. 2.3.2 or 2.3.5, the admixture of the OPW functions was obtained through the application of perturbation theory using a pseudopotential. The wave-function $\psi_{\boldsymbol{k}_F}(\boldsymbol{r})$ by this procedure, when used in (44), led to a value [152] of 14.8 for $\alpha(\boldsymbol{k}_F)$ in the $\langle 111 \rangle$ direction. In a later investigation [153], the mixing of the OPW's was handled varionally as described in Sect. 2.3.5 through the use of a plane wave basis set and three different pseudopotentials. This procedure leads to linear combinations of plane wave wave functions from which the linear combination of OPW functions are derived, see Section 2.3.5. The values obtained [153] for $\alpha(\boldsymbol{k}_F)$ for the three different pseudopotentials were 5.8, 6.4 and 6.2. None of these earlier calculations appear to have incorporated antishielding effects. The three values from the later procedure [153] appear to be significantly smaller than our OPW results, at least part of the difference perhaps being related to the influence of antishielding effects included in our work. The difference with the other linear combination of OPW investigation [152] is in the other direction. It is not possible to explain the latter difference as due to the antishielding effect, since this effect is expected to increase the enhancement factor further beyond the value for $\alpha(\boldsymbol{k}_F)$, which is already somewhat larger than our OPW result.

For copper, an earlier value of $\alpha(\boldsymbol{k}_F)$ had been obtained [121] using TB functions based on 3 s, 3 p and 3 d orbital states. This result, -6.5, was rather small and had opposite sign as compared to (61). No antishielding effects were included in this earlier work. We feel that the reasons for the strong difference between this result and ours is a consequence of both the neglect of antishielding effects as well as the limited nature of the basis set employed for the TB calculation. For the TB representation of the conduction band electrons wave-functions which are rather delocalized in this metal, one would need a much larger basis set, including especially 4 p, 5 p, and higher orbitals which can make important contributions to the EFG.

Using our values of $\alpha(\boldsymbol{k}_F)$ for Cu and Al in (60) and (61) and the expression (47) for the valence contribution to the EFG, we have obtained the EFG at the nearest neighbour ^{63}Cu and ^{27}Al sites in the presence of the interstitial μ^+, see Table 3. The result for $\delta\varrho(\boldsymbol{r})$ in (47) were taken [154] from a recent calculation [136] in which the perturbation of the charge density was obtained by the non-linear response procedure, with the impurity at the origin and the potential due to the surrounding ions replaced by a spherical average of the pseudopotentials associated with the ions in the host lattice, referred to as the spherical solid approximation as discussed in Section 3.1.

It appears from Table 3 that there is reasonable agreement between the theoretical valence contribu-

Table 3. Electric field-gradients at nearest neighbour nuclei due to valence contributions [a] in aluminium and copper.

System	OPW	APW	Experiment
μ^+ in Al	17.5	12.9	8.6 [b]
μ^+ in Cu	−46.8	−38.0	13.0 ± 7.2 [c]

[a] In units of 10^{13} esu/cm^3; [b] Ref. [108]; [c] Ref. [109].

tions in Al and the experimental result while the theoretical result for Cu is substantially overestimated compared to experiment.

As mentioned earlier in this section, the size effect contributions to the EFG from the lattice distortion effects have recently been evaluated [136] using (53) and (56), with the strain coefficients ε_{ij} (54) derived using the oscillatory expression (58) for the displacement vectors. The empirical parameter A in (58) was determined from ab initio calculations for interstitial hydrogen and muonium impurities [144, 145] as discussed in Sect. 3.1, the phase angle θ being obtained from elastic theory [142]. The other empirical parameters λ for aluminium and copper were estimated [136] by fitting the predicted and experimental EFG's at the fourth nearest neighbour ^{27}Al and ^{53}Cu nuclei of vacancies [102, 110] in these metals. The size effect contributions obtained in this manner were $16.0 \cdot 10^{13}$ and $30.2 \cdot 10^{13}$ esu/cm^3 respectively. These combined with the valence contributions, would lead to net EFG's in Al of $33.5 \cdot 10^{13}$ and $28.9 \cdot 10^{13}$ esu/cm^3 respectively, using the OPW and APW results in Table 3 and $-16.6 \cdot 10^{13}$ and $-22.0 \cdot 10^{13}$ esu/cm^3 respectively for Cu. It thus appears that the size effect contribution improves the agreement with experiment in Cu and worsens it for Al. It would be helpful to have values for the size effect contribution using [128] a summation over the ionic charges as in the first term in (1), with the positions of the ions in the distorted lattice obtained from ab initio calculations. This would allow one to avoid having to use the empirical parameter λ and also obviate the question of how well the ionic displacements can be fitted with (58).

In attempting to draw conclusions about the accuracy of the procedures proposed for size and valence effect contributions it is necessary to take account of not only the results discussed here for the muon problem but also those from a number of calculations that have been performed in the literature on vacancies in Al [128, 132, 136] and Cu [136] and dilute alloys with Al [131, 135] and Cu [124] as hosts. Instead of presenting and discussing these results, we shall touch on a few of their features in assessing the accuracy of the different procedures proposed and used in the literature for these two effects.

The first general conclusion that one can draw about these procedures is that they are certainly useful from a semi-quantitative point of view since they provide better than order of magnitude agreement with experiment in a number of instances. Looking at this question a little deeper, let us consider the valence contribution first. Of the two methods used in the literature to study density fluctuations, the self-consistent non-linear response procedure has the merit of being more first-principle in nature and of incorporating self-consistency within the framework of the model it uses. However, it has the deficiency of not incorporating the discrete nature of the surrounding arrangement of ions in the lattice. The scattering procedure is not first-principle in nature but does have the influence of the lattice included partially in an indirect way through the use of experimental resistivity data. A detailed quantitation inter comparison of results by the two procedures would be very helpful. Both these procedures predict that in the alloy system with Al host and vacancy in Al, the valence contribution is substantially smaller compared to the contribution from size effect. It would be interesting to compare the valence contributions from the scattering theory procedure with those from the non-linear response procedure for vacancy in Cu where at least for the first and fourth nearest neighbours, the valence contributions by the latter procedure are found to be larger than the size effect contributions. For the situations of muon in Cu and Al, the valence contributions from the latter procedure are also found to be rather important as discussed in this section and a comparison with results obtained by the scattering procedure would be interesting.

It should also be mentioned that while the dependence of $\varrho(\boldsymbol{r})$ on lattice distortion can be incorporated through the Blatt correction to Friedel sum rule mentioned earlier and by considering the density fluctuation $\delta\varrho(\boldsymbol{r})$ at displaced host ion positions, these may not be sufficient by themselves for the host nuclei. The EFG tensor around a host nucleus is sensitively dependent on the anisotropy of $\varrho(\boldsymbol{r})$ around it. It is our feeling that any model that has the impurity as the center, in handling the density fluctuation $\delta\varrho(\boldsymbol{r})$, does not give the vicinity of the host ion enough importance to be able to provide an accurate analysis of the dependence of the anisotropy around the host nucleus on the movement of the ion containing the nucleus in question and its neighbours from their equilibrium position. An improved treatment of $\delta\varrho(\boldsymbol{r})$, incorporating the discreteness of

the real lattice, which is warranted by the sizeable differences observed between experimental and theoretical EFG's in the Al-muon and Cu-muon systems discussed in this Section and similar differences in the Cu-vacancy system, should also include a careful analysis of the anisotropy of $\delta\varrho(\boldsymbol{r})$ about host ion nuclei. It would be interesting to see if improved treatments of $\delta\varrho(\boldsymbol{r})$ verify, or disagree with the conclusions about the smallness of the valence contributions in alloy and vacancy systems involving Al, as pointed out earlier.

Concerning the procedures in current use for studying the size effect using displacement vectors of the form in (49) the wide range of values of the empirical parameter λ needed to fit experimental data for different neighbours and different impurities makes the model appear to be unsatisfactory. The direct summation procedure avoids the need for any empirical parameters and seems in principle to be the most preferable of the three methods discussed in this section. It however is based on ab initio calculated results for the lattice displacements which are currently available for only a few systems. As far as the oscillatory displacement procedure is concerned, while the cosine form in (58) is by no means a rigorous one, this procedure is to be preferred over the other empirical procedure, because it uses fits to results for the ion displacements from ab initio investigations, thus making it have some similarity with the direct summation procedure. A comparison between these latter two procedures is possible in the case of the Al-vacancy system [128, 136]. Unfortunately the individual components for the size effect contribution to the EFG tensor have not been listed for the oscillatory displacement procedure. But for the second nearest neighbours, where the EFG tensor is axially symmetric one can compare the q^{s}_{zz} in the two cases and they compare very well, $9.6 \cdot 10^{13}$ esu/cm^3 for the direct summation procedure [128] and $8.8 \cdot 10^{13}$ esu/cm^3 for the oscillatory displacement [136] model.

However, the substantial difference between theory and experiment for ^{27}Al nuclei in the muon-Al system, and the less substantial, but significant difference between theory and experiment for the muon-Cu system discussed in this section as well as the significant differences found for the Cu-vacancy system and a number of Al alloy systems, suggest the need for improvements in the treatment of size effect as well as valence effects. It seems to us that the major need for improvement in the case of size effects lies in the evaluation of lattice distortion effects in a manner that is self-consistent with the electronic perturbations due to the presence of the impurity. Possible ways that this can be done will be discussed in the conclusions section.

3.3. Description of sources contributing to the electric field-gradients at solute nuclei in non-cubic metallic systems

As mentioned in the Introduction to Sect. 3, experimental data on the NQI at solute nuclei in dilute alloys are obtained primarily from nuclear radiative techniques such as ME [6], PAC [3] and a number of others including nuclear orientation [156] and β-decay NMR [157]. With these techniques, one studies NQI in excited nuclear states an to extract EFG's from the measured NQCC's, a knowledge of Q in the excited states is needed. This knowledge can be acquired by measurements [158] of the ratios of the coupling constants for the excited and ground nuclear states (the latter from conventional NMR or NQR measurements) or between excited states of two nuclei [159], one of which has a known Q. Additionally the Q's of excited nuclear states can also be obtained from accurate calculations of the EFG's in relatively simpler systems like diatomic molecules [29, 30] or pure metals [160, 161] where NQCC data for the nuclear excited states are available. A large volume of data has accumulated [104, 162] for a number of solute nuclei in different hosts from radiative measurements. An examination of the EFG's including derived from these data, primarily for hcp metal hosts has led to the empirical relation (35) discussed in Section 2.5.

The relation (35) as well as departures [104] from it and the dependency of these departures on the formal charges on the impurity ion in the host lattice have been used [164] for qualitative discussions of factors that could influence the EFG at solute nuclei. But to our knowledge no ab initito quantitative analyses of contributions to the EFG's at solute nuclei in non-cubic hosts has been published.

One can obtain insights into the sources that can contribute to these EFG's from the analyses of the corresponding sources for pure metals and host

nuclei in imperfect cubic alloy systems discussed in Sects. 2, 3.1, and 3.2.

The simplest approximation one can make as a starting point for determining the anisotropy of $\varrho(\boldsymbol{r})$ about the impurity nucleus in a dilute alloy is that the potential remains unchanged at all other regions of the system except the core region of the solute ion. In this latter region, the potential experienced by the core electron may be taken as corresponding to that for the free solute ion. In such a case a good approximation for the conduction electron wave functions in the vicinity of the impurity atom would, in the OPW approach, involve [165] taking a linear combination of OPW functions as in (4), with the coefficients $c_{\boldsymbol{k}+\boldsymbol{g}_i}$ the same as in the host lattice. However, the TB Bloch functions $\psi_{c,\boldsymbol{k}}(\boldsymbol{r})$ for the core states in (5), will involve $\Phi_c(\boldsymbol{r}-\boldsymbol{r}_s)$ (see (2) for explanation of this notation) for the impurity ion when $\boldsymbol{r}_s$ is the impurity site and the core states for the host ions for all other sites. The lattice of course is undistorted in this approximation. The contributions [165] from this mechanism to the EFG for alloys involving Cd as host metal are discussed in the next section and compared with experiment.

Among other mechanisms that could influence the EFG at the solute nucleus is the perturbation of $\varrho(\boldsymbol{r})$ outside the core region of the impurity produced by the change in the potential due to the presence of the impurity. This effect would be reflected in the OPW approximation by changes in the coefficients $c_{\boldsymbol{k}+\boldsymbol{g}_i}$ in (4). These changes would be transferred to $\varrho(\boldsymbol{r})$ in the vicinity of the nucleus through (see subsection 2.2.2) the impurity core components of the OPW functions in (5). It should be noted that the difference between the density at the impurity site arising from the combination of the two effects just discussed and the density one would find at the same site in the perfect host metal (with the impurity ion replaced by the host ion) is the counterpart of the density fluctuation $\delta\varrho(\boldsymbol{r})$ discussed in Sect. 3.1 which is pertinent for the EFG's for host nuclei in imperfect cubic metals. In the present case, we need the density at the impurity site itself and $\delta\varrho(\boldsymbol{r})$ is expected to represent a substantially larger change than that at the host sites discussed in Section 3.1. The procedures discussed there are not expected to be suitable here for the following reasons. The scattering procedure will not be suitable because in looking for the density at the origin itself, one will need many more phase shifts than the two, namely s and p phase shifts that have been used before. The non-linear response procedure would be rather complicated to use because one will now need the anisotropy in the electron density at the origin and to obtain this one would have to carry out the calculations over a volume whose shape reflects the non-cubic symmetry of the lattice rather than the spherical volume used for unperfect cubic metals. In addition, a departure from the spherical solid model for the potential arising from the ions surrounding the impurity will be needed to reflect the non-cubic symmetry of the environment which also would make the determination of $\delta\varrho(\boldsymbol{r})$ much more complicated.

The influence of the distortion of the lattice from the perfect metal structure will also have to be considered both because it can affect the lattice contribution to the EFG at the impurity site as well as the electron density distribution at the impurity site. The latter would be somewhat more difficult to study than in the case of the host nuclear systems discussed in Section 3.1. However this type of change in $\varrho(\boldsymbol{r})$ is expected to be relatively unimportant for the impurity site in the present class of systems because of the expected dominance of the contribution to the density from the first two effects just discussed. It should also be pointed out that elastic continuum procedures, of the types discussed in Sect. 3.1 (for the ionic contribution to the EFG from lattice distortion effects), would be rather complicated to apply to the present systems because of the non-cubic symmetry of the host lattice. One would have to obtain the displaced lattice positions instead from ab initio calculations of the type performed for impurities in cubic metals such as Al and apply the direct summation procedure.

3.4. Electric field-gradients at nuclei of substitutional impurities in cadmium-based alloys

In the present section, we shall discuss the results of an investigation of [165] the first mechanism discussed in Sect. 3.3 and the lattice contribution, ignoring effects of lattice distortion, for three alloy systems involving Zn, In, and Sn impurities in Cd. There were two major motivations for these investigations. One was to study how these contributions and their relative strengths varied from one impurity to another, since the formal charges on the impurity ions changed systematically from being

zero for the host ion for Zn to + 1 and + 2 respectively for In and Sn solutes. The second aim was to compare the sum of these two contributions to the EFG with experimental values [105–107] from measurements by radiative techniques, and to draw conclusions from the differences between theory and experiment about the importance of other mechanisms that contribute to the EFG.

The lattice contribution was obtained by the same procedure as in the case of the pure metals (Sect. 2.5), the antishielding factors employed now being those corresponding to the impurity ions. Since lattice distortion effects were not included, the unshielded value of the EFG at the impurity nucleus was the same as in pure Cd, obtainable using the equation available in the literature [71] for the dependence of the EFG on the c/a ratio. The antishielding factors for the Zn^{2+} and In^{3+} impurity ions were obtained [166] by the usual perturbation procedure [167] involving solution of the first-order perturbation equations for the core wave-functions in the presence of the perturbation potential due to Q. The wave-functions used for the core states corresponded to those for the neutral atoms so as to at least approximately incorporate the influence [168] of the potential due to the conduction electrons. The values of $\gamma_\infty(Zn^{2+})$ and $\gamma_\infty(In^{3+})$ obtained in this way were -14.0 and -27.0 respectively. For Sn^{4+}, no value is available for γ_∞ using core states corresponding to neutral Sn atom. The available value [169] of -22.3 for γ_∞ for Sn^{4+} was therefore utilized, the experience with Zn and In suggesting that the expected reduction in the magnitude of this value in going to cores in neutral Sn atom would not be significantly larger than 1.0.

For the evaluation of the conduction electron contributions to the EFG, the same procedure was followed as for pure Cd metal (Section 2.5). The linear combination of plane waves obtained [52] from the pseudopotential for cadmium however was now orthogonalized [166] to Zn^{2+}, In^{3+} and Sn^{4+} core functions for the three alloy systems to obtain the corresponding linear combinations of OPW functions. The influence of antishielding effects for the conduction electrons could have been included by the first-principle procedure described in Section 2.4. However, to avoid the substantial effort that this would entail, the same approximate procedure was employed at that used [146] for muon in Al and Cu.

Table 4. Electric field-gradient[a] at impurity nuclei in cadmium-based alloys.

Alloy system	Lattice contribution	Electronic contribution	Total	Experimental electric field-gradient
ZnCd	−54.4	154.9	100.5	$\lvert 95.6 \pm 9.6 \rvert$ [b]
InCd	−101.6	346.8	245.2	313 ± 29 [c]
SnCd	−84.9	300.7	215.8	$\lvert 263 \pm 57 \rvert$ [d]

[a] The electric field-gradients are all expressed in units of 10^{13} esu/cm^3.
[b] From Ref. [105] using $Q(^{67}Zn,\ I = 9/2) = 0.57$ barns (Ref. [170]).
[c] From Ref. [106] using $Q(^{117}In, I = 9/2) = -0.62$ barns (Ref. [171]).
[d] From Ref. [107] using $Q(^{113}Sn, I = 11/2) = \pm 0.46$ barns (Ref. [172]).

Table 4 presents the lattice and conduction electron contributions and their sums for the three alloy systems [165]. The experimental values of the EFG's were obtained by combining the measured values [105–107] of the NQCC's for the excited nuclear states ^{67}Zn ($I = 9/2$), ^{117}In ($I = 9/2$), and ^{113}Sn ($I = 11/2$) of the impurities in the three alloy systems with their Q. For the In solute, the sign of the NQCC was available [106], while for the other two cases, the signs were not known [105, 107]. The Q's for the three excited nuclear states utilized in these measurements were taken from the literature [170–172], these values being 0.57, -0.62 and ± 0.46 barns respectively.

From Table 4, it is encouraging to note that the theoretical and experimental values of the EFG's at the impurity nuclei are in reasonable agreement with each other. This suggests that the two mechanisms considered here represent the major contributors to the EFG at the impurity nucleus. It is interesting in this respect that for the Zn^{2+} impurity, which has the same charge as the host Cd^{2+} ion, theory and experiment agree within the error range of the experimental result while for In^{3+} and Sn^{4+} impurities which carry formal charges + 1 and + 2 higher than the Cd^{2+} ion, the experimental EFG are about 21% and 18% higher than theory. This behaviour could, as discussed in Sect. 3.3 be due to perturbations in the electron distributions as well as lattice distortions produced by the larger charges on the In^{3+} and Sn^{4+} impurities. Considering the first, we have assumed that the linear combinations of plane-waves for the pseudo-functions for both the impurity systems are the same as for

the pure metal. In view of the changed potentials experienced by the conduction electrons due to the larger charges on In^{3+} and Sn^{4+}, it is not unexpected that there would be changes in the pseudo-functions as well as the Fermi volumes and surfaces, as determined by the occupied regions of the energy bands in the latter two systems. Additionally, the larger formal charges could lead to changes in the positions of the host ions, as well as the impurity ion in the lattice as compared to the lattice in perfect Cd metal. This lattice distortion would be expected to lead to changes in the lattice contributions in the EFG as well as some changes in the electronic contribution due to changes in the conduction electron wave-functions. In addition, of course, the different sizes of the Zn^{2+}, In^{3+} and Sn^{4+} ions as compared to the host Cd^{2+} could also lead to lattice distortions, analogous to the effect discussed in Section 3.1.

It will be interesting to explore these additional effects in the future, the fact that there is significant cancellation between the electronic and lattice contributions in Table 4 suggesting that relatively small changes in either could improve the agreement between theory and experiment for the two latter impurity systems. The departure from experiment is a little weaker for the Sn impurity than for In, while the reverse would have been expected on the basis of the formal charges on their ions in the Cd lattice. This feature may be a result of the increased cancellation between the contributions to the EFG from the perturbation effects on the conduction electron distribution and the distortion of the lattice produced by the extra charges in the case of Sn^{4+} as compared to In^{3+}. It would be interesting to examine this possibility.

Before terminating this section, it is worthwhile making two remarks. The first is that, as in the case of pure metals, both the lattice and conduction electron contributions are subject to, though in varying measures, the antishielding effects associated with the impurity ion. This provides qualitative support for the empirical relation in (35) derived from examination of NQI data for impurity nuclei in alloy systems. The second point to note is that it is not unexpected that approximate treatments of the EFG's at impurity nuclei in non-cubic hosts can provide better agreement with experiment than for host nuclei in cubic metals in presence of impurity ions. This is because, even in the absence of electronic perturbation and lattice distortion effects, there is already a sizeable contribution to the EFG at the impurity nucleus because of the non-cubic symmetry of the host lattice. In the case of alloy systems involving cubic hosts, however, the host nuclei experience finite EFG's only because the cubic symmetry around them is destroyed by lattice distortion and electronic perturbation effects due to the presence of the solute atom.

4. Concluding Remarks

From the results and discussions dealing with pure metals it appears that theory is able to provide satisfactory explanations of the experimentally observed NQCC's. However, for this purpose, one needs to include all the important physical effects and have an accurate knowledge of all the factors involved, including the conduction electron wave-functions for the entire occupied volume in $\boldsymbol{k}$-space below the Fermi-surface, the appropriate antishielding effects for the ionic and conduction electron contributions to the EFG's and of course the Q of the nucleus involved.

There is a need for additional efforts in two areas to further enhance our understanding of the EFG's in pure metals. The first concerns the comparison of the electronic contribution to the EFG's obtained by different methods, such as the OPW and APW procedures which have been applied to Be, where one needs to develop ways to improve the accuracy of the individual procedures. The other direction is to try for at least one metal first-principle self-consistent HF-calculations of the band structure as has been done [44] in ferromagnetic metals and then apply a many-body perturbation procedure that has been adapted to metallic systems [173]. These investigations would allow one to draw conclusions about the effects of departures from the HF approximation in the commonly used OPW and APW approaches and the influence of many-body effects which has been tested and found to be not so important for antishielding phenomena [174], but whose effects on the direct contributions from the conduction electrons has not yet been tested.

Another area in which it would be helpful to see some efforts in the future is the application of HF cluster approaches [86], especially for semimetals, where TB and approximate cluster procedures have

been found [78, 84] to be reasonably successful. The testing of these procedures would be desirable for eventual applications to the EFG associated with impurities in semi-metals and for surfaces [175].

In the area of temperature dependence of EFG's in pure metals, it would be helpful to have analyses in other metals of all the possible contributions as has been done [92] for Zn and Cd metals. In particular, it will be interesting to carry out such investigations in the tetragonal face centered In metal, where c/a is nearly unity and hence changes in contributions from anharmonic phonon effects, leading to changes in the c/a ratio, would be expected to particularly influence the EFG.

As far as the field of alloys is concerned, the situation especially for the EFG's at host nuclei in cubic metals, is still unsettled. The valence and size effects and their interactions considered in the literature are undoubtedly the correct mechanisms. However, there are a number of improvements still needed for the evaluation of the contributions from these mechanisms. In the treatment of size effect contributions, there is need to move away from parametric treatments to more first-principle analyses which recognize the discrete nature of the lattice. An improvement is needed in the treatment of the anisotropy of $\varrho(\boldsymbol{r})$ around the host nuclei. The treatments of the perturbation of $\varrho(\boldsymbol{r})$ using the impurity site as the origin are not expected to be sufficiently sensitive to the question of the anisotropy about the host nuclear sites. It will be helpful to obtain the change in potential experienced by the conduction electrons using the already obtained perturbations of $\varrho(\boldsymbol{r})$ and displacements of host ions. The influence of this changed potential, taking carefully into account its anisotropy, can then be handled by various orders of perturbation theory or variationally, to analyze the additional anisotropic distortion it produces in $\varrho(\boldsymbol{r})$ around the nuclei, allowing an enhancement in the self-consistency of the electronic contribution to the EFG's at host nuclei.

Another area in which additional effort is needed is in the incorporation of self-consistency between the electronic density perturbation and lattice distortion. It will be useful to carry out self-consistent cluster calculations [86], simulating the infinite lattice by a sizeable cluster of atoms including the impurity atom and minimising the total energy of the cluster as a function of the positions of the ions. This would entail very sizeable computational efforts which would probably require the use of a supercomputer or massively parallel processor [176], but it would provide some useful answers regarding the dependence of the lattice distortion on the electronic perturbation and vice versa.

In summary, the NQI in metallic systems, perfect and imperfect, has already proven to be a very valuable tool in assessing the correctness of our knowledge of the structure of these systems at atomic and electronic levels. It is hoped that this review will stimulate additional efforts using some of the suggestions made here as well as by alternative channels to further enhance the viability of this nuclear property as a tool for study of solid state systems in general and metals and alloys in particular.

Acknowledgement

The authors are very grateful to Professor Dr. Alarich Weiss for many valuable discussions. We are also deeply grateful to Mr. Narayan Sahoo for many helpful suggestions and discussions. The collaborative effort for this work was supported by NATO Research Grant No. 496/84.

[1] E. R. Andrew, Nuclear Magnetic Resonance, Cambridge University Press, Cambridge 1955; A. K. Saha and T. P. Das, Theory and Applications of Nuclear Induction, Saha Institute of Nuclear Physics, Calcutta 1955; A. Abragam, The Principles of Nuclear Magnetism, Oxford University Press, London 1961; C. P. Slichter, Principles of Magnetic Resonance, Harper and Row, New York 1963.

[2] T. P. Das and E. L. Hahn, Nuclear Quadrupole Resonance Spectroscopy, Academic Press, New York 1957; E. A. C. Lucken, Nuclear Quadrupole Coupling Constants, Academic Press, New York 1969; Alarich Weiss, in: Advances in Nuclear Quadrupole Resonance, (J. A. S. Smith, ed.), Heyden, London 1974.

[3] H. Fraunfelder and R. M. Steffen, in: Alpha-, Beta-Gamma-Ray Spectroscopy, Vol. 2 (K. Siegbahn, ed.), North-Holland Publishers, Amsterdam 1965; W. D. Hamilton, Editor, The Electromagnetic Interactions in Nuclear Spectroscopy, North-Holland Publishers, Amsterdam 1975; R. D. Gill, Gamma-Ray Angular Correlations, Academic Press, New York 1975; H.-J. Behrend and D. Budnick, Z. Physik **168,** 155 (1962); R. S. Raghavan, P. Raghavan, and E. N. Kaufmann, Phys. Rev. Lett. **31,** 111, 802 (1973); O. Klepper, E. N. Kaufmann, and D. E.

Murnick, Phys. Rev. **C 7,** 1691 (1973); H. Haas, Phys. Scr. **11,** 221 (1975).
[4] E. Matthias, D. A. Shirley, M. P. Klein, and N. Edelstein, Phys. Rev. Lett. **16,** 974 (1966); T. Minamisono, K. Matuda, A. Mizobuchi, and K. Sugimoto, J. Phys. Soc. Japan **30,** 311 (1971); H. Ackermann, D. Dubbers, and H.-J. Stockmann, in: Advances in Nuclear Quadrupole Resonance (J. A. S. Smith, ed.), Vol. 3, London 1978.
[5] E. Matthias, B. Olsen, D. A. Shirley, J. E. Templeton, and R. M. Steffen, Phys. Rev. **A 4,** 1626 (1971); S. R. De Groot, H. A. Tolhoek, and W. J. Huiskamp, Alpha-, Beta-, and Gamma-Ray Spectroscopy (K. Siegbahn, ed.), Vol. 2, page 1199, North-Holland, Amsterdam 1965; P. T. Callaghan, N. J. Stone, and B. G. Turrell, Phys. Rev. **B 10,** 1075 (1974); G. Kaindl, F. Bacon, and A. J. Soinski, Phys. Lett. **B 46,** 62 (1973); E. Ernst, E. Hagn, E. Zech, and G. Eska, Hyperfine Inter. **4,** 581 (1978).
[6] G. K. Wertheim, Mössbauer Effect; Principles and Application, Academic Press, New York 1964; I. J. Gruverman, Editor, Symposium on Mössbauer Effect Methodology, 3, Plenum Press, New York 1967; Applications of Mössbauer Effect, Proceedings of International Conference on Mössbauer Effect, Leuven, Belgium, September 1985, Hyperfine Interactions (1986) (to be published).
[7] M. H. Cohen and F. Reif, in: Solid State Physics, Vol. 5, (F. Seitz and D. Turnbull, ed.), Academic Press, New York 1957; T. P. Das and E. L. Hahn, Ref. [2].
[8] N. C. Mohapatra, C. M. Singal, and T. P. Das, Phys. Rev. Lett. **31,** 530 (1973).
[9] See for instance R. M. Sternheimer, Phys. Rev. **130,** 1423 (1963); **132,** 1637 (1963) and Z. Naturforsch. **41 a,** 24 (1986); P. C. Schmidt, K. D. Sen, Alarich Weiss, and T. P. Das, Phys. Rev. **B 22,** 4167 (1980).
[10] H. M. Foley, R. M. Sternheimer, and D. Tycko, Phys. Rev. **93,** 734 (1954); R. M. Sternheimer, Phys. Rev. **146,** 140 (1966); E. H. Hygh and T. P. Das, Phys. Rev. **143,** 452 (1966); P. C. Pattnaik, M. D. Thompson, and T. P. Das, Phys. Rev. **B 16,** 5390 (1977); K. K. P. Rao and N. C. Mohapatra, Phys. Rev. **A 24,** 10 (1981); K. D. Sen, P. C. Schmidt, and Alarich Weiss, Z. Naturforsch. **41 a,** 37 (1986).
[11] H. Schüler and T. Schmidt, Z. Physik **94,** 457 (1935).
[12] N. F. Ramsey, Molecular Beams, Oxford University Press, London 1955.
[13] See for instance: R. Neugart, F. Buchinger, W. Klempft, A. C. Mueller, E. W. Otten, C. Ekstrom, and J. Heinemeier, Hyperfine Inter. **9,** 151 (1981); A. C. Mueller, F. Buchinger, W. Klempt, E. W. Otten, R. Neugart, C. Ekstrom, and J. Heinemeier, Nucl. Phys. **A 403,** 234 (1983).
[14] S. N. Ray, T. Lee, and T. P. Das, Phys. Rev. **A 8,** 1748 (1973); J. E. Rodgers and T. P. Das, Phys. Rev. **A 12,** 353 (1975); S. N. Ray, T. Lee, and T. P. Das, Phys. Rev. **B 16,** 4794 (1977); J. E. Rodgers, R. Roy, and T. P. Das, Phys. Rev. **A 14,** 543 (1976).
[15] R. M. Sternheimer and R. F. Pierls, Phys. Rev. **A 4,** 1722 (1971).
[16] R. M. Sternheimer, Phys. Rev. **164,** 10 (1967).
[17] R. M. Sternheimer, Phys. Rev. **84,** 244 (1951); see also G. D. Gaspari, W. M. Shyu, and T. P. Das, Phys. Rev. **134,** A 852 (1964).
[18] T. P. Das and R. Bersohn, Phys. Rev. **102,** 733 (1958).
[19] See for instance: E. S. Chang, R. T. Pu, and T. P. Das, Phys. Rev. **174,** 1, 16 (1968); J. Andriessen, K. Raghunathan, S. N. Ray, and T. P. Das, Phys. Rev. **B 15,** 2533 (1977); M. Vajed-Samii, J. Andriessen, S. N. Ray, and T. P. Das, Phys. Rev. **A 20,** 1787 (1979).
[20] See references in Ref. [14].
[21] S. N. Ray et al. (1973); J. E. Rodgers et al. (1975), Ref. [14].
[22] P. Buck, I. I. Rabi, and B. Senitzky, Phys. Rev. **104,** 553 (1956) and references therein; R. W. Schmieder, A. Lurio, and W. Happer, Phys. Rev. **173,** 76 (1968).
[23] A. G. Blachmann and A. Lurio, Phys. Rev. **153,** 164 (1967); A. Lurio, Phys. Rev. **126,** 1768 (1962); N. S. Laulinen and M. N. McDermott, Phys. Rev. **177,** 1606 (1969).
[24] N. F. Ramsey, Ref. [12].
[25] C. H. Townes and A. L. Schawlow, Microwave Spectroscopy, McGraw-Hill Book Company, New York 1955.
[26] K. Sugimoto, A. Mizobuchi, and K. Nakai, Phys. Rev. **134,** B 539 (1964); see also W. Kreische, H. U. Maar, H. Niedrig, K. Reuter, and K. Roth, Hyper. Inter. **4,** 732 (1978); K. Bonde-Nielsen and B. Toft, in: Proceedings of the Fifth International Conference on Hyperfine Interactions, Berlin (1980), (G. Kaindl and H. Haas, ed.), North-Holland Publishers, Amsterdam 1981; for measurements on ground-state of ^{20}F ($I = 2$), see F. Fujara, H.-J. Stockmann, H. Ackermann, W. Buttler, H. Grupp, P. Heitjans, G. Kiese, and A. Korblein, Z. Physik **B 37,** 151 (1980).
[27] T. K. McNab, D. H. W. Carstens, D. M. Gruen, and R. L. McBeth, Chem. Phys. Lett. **13,** 600 (1972); F. J. Litterst, A. Schichl, and G. M. Kalvius, Chem. Phys. **28,** 89 (1978).
[28] G. K. Wertheim et al., Ref. [6].
[29] K. C. Mishra, K. J. Duff, and T. P. Das, Phys. Rev. **B 25,** 3389 (1982).
[30] K. J. Duff, K. C. Mishra, and T. P. Das, Phys. Rev. Lett. **46,** 1611 (1981).
[31] C. T. O'Konski and T. K. Ha, J. Chem. Phys. **49,** 5354 (1968).
[32] K. Raghunathan, S. N. Ray, J. Andriessen, and T. P. Das, Phys. Rev. Lett. **44,** 312 (1980).
[33] B. Jeckelmann, W. Beer, I. Beltrami, F. W. N. De Boer, G. de Chambrier, P. F. A. Goudsmit, J. Kern, H. J. Leisi, W. Ruckstuhl, and A. Vacchi, Nucl. Phys. **A 408,** 495 (1983).
[34] P. Brix, Z. Naturforsch. **41 a,** 3 (1986).
[35] M. D. Thompson, P. C. Pattnaik, and T. P. Das, Phys. Rev. **B 18,** 5402 (1978).
[36] E. Bodenstedt and B. Perscheid, Hyperfine Inter. **5,** 291 (1978); E. Bodenstedt, B. Perscheid, and S. Nagel Z. Physik B, in press (1986) and references therein.
[37] J. R. Reitz, in: Solid State Physics, Vol. 1, (F. Seitz and D. Turnbull, ed.), Academic Press, New York 1955.
[38] C. Herring, Phys. Rev. **57,** 1169 (1940); T. O. Woodruff, in: Solid State Physics, (F. Seitz and D. Turnbull, ed.), Academic Press, New York 1957; G. D. Gaspari and T. P. Das, Phys. Rev. **167,** 660 (1968).
[39] J. C. Slater, Phys. Rev. **81,** 385 (1951); W. Kohn and L. J. Sham, Phys. Rev. **140,** A 1133 (1965); K. Schwarz, Phys. Rev. **B 5,** 2466 (1972).
[40] M. Pomerantz and T. P. Das, Phys. Rev. **119,** 70 (1960); G. D. Gaspari and T. P. Das, Ref. [38].
[41] T. L. Loucks, Augmented Plane Wave Method: A Guide to Performing Electronic Structure Calculations, W. A. Benjamin, New York 1967.
[42] P. Blaha, K. Schwarz, and P. Herzig, Phys. Rev. Lett. **54,** 1192 (1985).

[43] P. C. Schmidt, P. C. Pattnaik, and T. P. Das, Phys. Rev. **B 29,** 3066 (1984).
[44] K. J. Duff and T. P. Das, Phys. Rev. **B 3,** 192, 2294 (1971); Phys. Rev. **B 12,** 3870 (1975); C. M. Singal and T. P. Das, Phys. Rev. **B 16,** 5068, 5093 (1977); C. M. Singal, B. Krawchuk, and T. P. Das, Phys. Rev. **B 16,** 5108 (1977); N. C. Mohapatra, Ph.D. Thesis, State University of New York at Albany 1976; T. P. Das, Hyperfine Inter. **6,** 53 (1979).
[45] W. A. Harrison, Theory of Pseudopotentials, W. A. Benjamin, New York 1960; Phys. Rev. **181,** 1036 (1969); J. A. Moriarty, Phys. Rev. **B 1,** 1363 (1970).
[46] M. D. Thompson, G. Ciobanu, and T. P. Das, Phys. Rev. **B 19,** 4328 (1979); P. C. Pattnaik, M. D. Thompson, and T. P. Das, Phys. Rev. **B 19,** 4326 (1979); P. Jena, S. D. Mahanti, and T. P. Das, Phys. Rev. **B 2,** 2264 (1970).
[47] R. W. Stark and L. M. Falicov, Phys. Rev. Lett. **19,** 795 (1967).
[48] W. A. Harrison (1969) Ref. [45]; J. A. Moriarty, Ref. [45]; M. D. Thompson, Ph.D. Thesis, State University of New York at Albany 1979 (unpublished); M. D. Thompson, G. Ciobanu, and T. P. Das, to be published.
[49] G. B. Bachelet, D. R. Hamann, and M. Schlüter, Phys. Rev. **B 26,** 4199 (1982); W. R. Wadt and P. Jeffrey Hay, J. Chem. Phys. **82,** 270, 284, 299 (1985).
[50] P. C. Pattnaik et al. Ref. [45]. The empirical pseudopotential of Stark and Falicov (Ref. [47]) for zinc was used in this work.
[51] P. Jena, S. D. Mahanti, and T. P. Das, Phys. Rev. **B 1,** 432 (1970).
[52] M. D. Thompson et al., Ref. [45]. The Harrison-Moriarty pseudopotential (Ref. [45]) was used in this work.
[53] N. C. Mohapatra, P. C. Pattniak, M. D. Thompson, and T. P. Das, Phys. Rev. **B 16,** 3001 (1977).
[54] R. M. Sternheimer et al. (1954) Ref. [10]; R. M. Sternheimer (1966), Ref. [10]; K. D. Sen et al., Ref. [10]; K. K. P. Rao and N. C. Mohapatra (1981), Ref. [10].
[55] P. C. Pattniak et al., Ref. [10].
[56] R. S. Raghavan, E. N. Kaufmann, and P. Raghavan, Phys. Rev. Lett. **34,** 1280 (1975); P. Raghavan, E. N. Kaufmann, R. S. Raghavan, E. J. Ansaldo, and R. A. Naumann, Phys. Rev. **B 13,** 2835 (1978).
[57] P. C. Schmidt et al., Ref. [43]; for earlier theoretical work on beryllium metal, see N. C. Mohapatra, C. M. Singal, T. P. Das, and P. Jena, Phys. Rev. Lett. **29,** 456 (1972) and P. Jena and J. Rath, Phys. Rev. **B 23,** 3823 (1981).
[58] P. Jena, S. D. Mahanti, and T. P. Das, Phys. Rev. **B 7,** 975 (1973).
[59] P. C. Pattnaik et al., Ref. [46].
[60] M. D. Thompson et al., Ref. [46].
[61] G. D. Gaspari and T. P. Das, Ref. [38]; M. D. Thompson, Ref. [48]; M. D. Thompson et al., Ref. [48]; K. W. Lodge, Phys. Lett. A **64,** 315 (1977); J. Phys. **F 8,** 447 (1978).
[62] D. E. Barnaal, R. G. Barnes, B. R. McCart, L. W. Mohn, and D. R. Torgeson, Phys. Rev. **157,** 510 (1967); W. T. Anderson, M. Ruhlig, and R. R. Hewitt, Phys. Rev. **161,** 293 (1967); H. Alloul and C. Froidevaux, J. Phys. Chem. Solids **29,** 1623 (1968); Y. Chabre and P. Segransan, Solid State Comm. **12,** 815 (1973).
[63] P. D. Dougan, S. N. Sharma, and D. L. Williams, Can. J. Phys. **47,** 1047 (1969).
[64] W. T. Vetterling and R. V. Pound, Amer. Inst. Physics Conf. Proc. **38,** 27 (1977).
[65] W. Potzel, A. Förster, and G. M. Kalvius, Phys. Lett. A **67,** 421 (1978).
[66] E. N. Kaufmann, J. R. Brookemann, P. C. Canepa, T. A. Scott, D. H. Rasmussen, and J. H. Perepezko, Solid State Comm. **29,** 375 (1978).
[67] J. Abart, E. Palangié, and J. Voitländer, J. Chem. Phys. **78,** 5468 (1983).
[68] R. S. Raghavan and P. Raghavan, Phys. Lett. **A 36,** 313 (1971); R. S. Raghavan, P. Raghavan, and E. N. Kaufmann, Phys. Rev. **C 12,** 202 (1975).
[69] For ^{9}Be, Q used is taken from the calculations of the EFG in the $2s\,2p(^3P)$ excited state by S. N. Ray et al., Ref. [14], including many-body effects and combined with the NQCC for this atomic state measured by A. Lurio, Ref. [23]; for ^{25}Mg, Q is obtained from the EFG in the $3s\,3p(^3P)$ excited state using the EFG derived from the empirical Fermi-Segre formula (H. Kopfermann, Nuclear Moments, Academic Press, New York 1958, page 123) combined with the measured NQCC for this state by A. Lurio, Ref. [23]; a many-body calculation of the EFG in the $3s\,3p(^3P)$ excited state of Mg atom is in progress (S. N. Ray and T. P. Das, to be published); for ^{67}Zn, Q is derived from the $4s\,4p(^3P)$ excited state measurement of N. S. Laulinen and M. N. McDermott, Ref. [23], with the EFG used for this purpose involving an approximate treatment of Sternheimer antishielding effects; for ^{111}Cd ($I = 4/2$) excited nuclear state, Q is obtained from measurements of the ratio of NQCC for Cd^{2+} and In^{3+} ions in ionic crystals (R. S. Raghavan, P. Raghavan, and J. M. Friedt, Phys. Rev. Lett. **30,** 10 (1973)).
[70] For Be^{2+}, the antishielding factor γ_∞ used is from T. P. Das and R. Bersohn, Ref. [18]; for Mg^{2+}, the γ_∞ used is from P. D. Dougan, S. N. Sharma, and D. L. Williams, Can. J. Phys. **47,** 1047 (1969); for Zn^{2+} and Cd^{2+}, the γ_∞ used are from a perturbation calculation by the Sternheimer procedure (Ref. [17]) of solving the first order perturbation equation by the differential equation approach and was carried out by N. C. Mohapatra, T. P. Das, R. M. Sternheimer, and D. Ikenberry, the values being quoted in Ref. [53]. For Zn^{2+}, the HF wave functions of neutral zinc were used to simulate the influence of the potential produced by the conduction electrons at the core electron sites. The antishielding factor of -14.0 obtained in this way was only 10 per cent larger in magnitude than for Zn^{2+} ion. For Cd^{2+}, the ionic HF wave functions were used.
[71] T. P. Das and M. Pomerantz, Phys. Rev. **123,** 2070 (1961).
[72] T. P. Das and M. Pomerantz, Ref. [71].
[73] C. Kittel, Ref. [35], page 24.
[74] A. Lurio, Ref. [23].
[75] R. S. Raghavan et al. Ref. [69].
[76] A. Coker, T. Lee, and T. P. Das, Phys. Rev. B **22,** 2968, 2976 (1980).
[77] P. Boolchand, T. Henneberger, and J. Oberschmidt, Phys. Rev. Lett. **30,** 1292 (1973).
[78] E. H. Hygh and T. P. Das, Phys. Rev. **143,** 452 (1966).
[79] R. R. Hewitt and B. F. Williams, Phys. Rev. **129,** 1188 (1963).
[80] B. F. Williams and R. R. Hewitt, Phys. Rev. **146,** 286 (1966).
[81] C. Kittel, Ref. [35], Chapter 8.

[82] J. Ketterson and Y. Eckstein, Phys. Rev. **132,** 1885 (1963) and references therein.
[83] G. Wannier, Phys. Rev. **52,** 191 (1937); see also J. Callaway, Energy Band Theory, Academic Press, New York 1964; Chapter 2.
[84] A. Coker, T. Lee, and T. P. Das, Phys. Rev. **B 13,** 55 (1976).
[85] M. van Rossum, G. Langouche, K. C. Mishra, and T. P. Das, Phys. Rev. **B 28,** 6086 (1983); M. van Rossum, I. Dezsi, G. Langouche, K. C. Mishra, A. Coker, and T. P. Das, Hyperfine Inter. **15–16,** 475 (1983).
[86] N. Sahoo, K. C. Mishra, A. Coker, C. K. Mitra, L. C. Snyder, A. Glodeanu, and T. P. Das, Phys. Rev. Lett. **50,** 913 (1983); N. Sahoo, K. C. Mishra, and T. P. Das, Phys. Rev. Lett. **55,** 1506 (1985); B. N. Dev, K. C. Mishra, W. Gibson, and T. P. Das, Phys. Rev. **B 29,** 1101 (1984).
[87] S. K. Mishra, K. C. Mishra, and T. P. Das, to be published.
[88] W. Körner, W. Keppner, B. Lehndorff-Junges, and G. Schatz, Phys. Rev. Lett. **49,** 1735 (1982).
[89] P. Heubes, G. Hempel, H. Ingwersen, R. Keitel, W. Klinger, W. Loeffler, and W. Witthuhn, in Contributed Papers Volume of "International Conference on Hyperfine Interactions Studied in Nuclear Reactions and Decay" (E. Karlson and R. Wäppling, ed.), Uppsala 1974, page 208; J. Christiansen, P. Heubes, R. Keitel, W. Klinger, W. Loeffler, W. Sandner, and W. Witthuhn, Z. Physik **B 24,** 177 (1976).
[90] P. Heubes et al., Ref. [89]; J. Christiansen et al., Ref. [89]. See also review article by E. N. Kaufmann and R. J. Vianden, Rev. Mod. Phys. **51,** 161 (1979).
[91] See for instance, E. N. Kaufmann and R. J. Vianden, Ref. [90], page 199.
[92] M. D. Thompson, P. C. Pattnaik, and T. P. Das, Phys. Rev. **B 18,** 5402 (1978); see also T. P. Das, Phys. Scr. **11,** 121 (1975), last paragraph.
[93] For a discussion of harmonic and anharmonic lattice vibrations, see C. Kittel, Ref. [35], Chapters 4 and 5. See also R. E. DeWames, T. Wolfram, and G. W. Lehman, Phys. Rev. **138,** A 725 (1965).
[94] D. Quitmann, K. Nishiyama, and D. Riegel, in: Magnetic Resonance and Related Phenomena (P. S. Allen, E. R. Andrew, and C. A. Bates, eds.), North-Holland, Amsterdam, page 349; P. Jena, Phys. Rev. Lett. **36,** 418 (1976); K. Nishiyama, F. Dimmling, Th. Kornrumpf, and D. Riegel, Phys. Rev. Lett. **37,** 357 (1976).
[95] P. Jena, Phys. Rev. **B 17,** 1046 (1978); P. Jena and J. Rath, Ref. [57].
[96] R. V. Kasowski and L. M. Falicov, Phys. Rev. Lett. **22,** 1001 (1969); R. V. Kasowski, Phys. Rev. **187,** 89 (1969); P. Jena, S. D. Mahanti, G. D. Gaspari, and T. P. Das, Phys. Rev. **B 1,** 1160 (1970); P. Jena and T. P. Das, Phys. Rev. **B 4,** 3931 (1971).
[97] R. S. Raghavan and P. Raghavan, Phys. Lett. **A 36,** 313 (1971); J. Bleck, R. Butt, H. Haas, W. Ribbe, and W. Zeitz, Phys. Rev. Lett. **29,** 1371 (1972).
[98] H. Bertschat, E. Recknagel, and B. Spellmeyer, Phys. Rev. Lett. **32,** 18 (1974).
[99] P. Raghavan, R. S. Raghavan, and W. B. Holzapfel, Phys. Rev. Lett. **28,** 903 (1972); T. Butz and G. M. Kalvius, Hyperfine Inter. **2,** 222 (1976); J. Y. Hwang, P. C. Canepa and T. A. Scott, J. Phys. Chem. Sol. **38,** 1403 (1977); J. DaJornada, E. R. Fraga, R. P. Livi, and F. C. Zawislak, Hyperfine Inter. **4,** 589 (1978).
[100] N. C. Mohapatra, C. M. Singal, and T. P. Das, Phys. Rev. Lett. **31,** 530 (1973) (see also slight correction to this work in T. P. Das, Ref. [92]). In this work a study is made of the change in lattice and electronic contributions to the EFG with lattice constant changes due to pressure to explain the pressure data in cadmium in P. Raghavan et al., Ref. [99]. K. Nishiyama and D. Riegel, Phys. Lett. **A 57,** 270 (1976) have also studied pressure dependence of the EFG using an empirical approach in which the role of the conduction electrons is considered to be one of screening the lattice contribution to the EFG's, leading to an amplification of the latter included through an amplification parameter. The same approach was used to study the temperature dependence of the EFG in K. Nishiyama et al., Ref. [94]. See also T. Butz, Hyperfine Inter. **4,** 528 (1978) a) for discussions about the origin of the pressure dependence of the EFG in metallic systems.
[101] N. Bloembergen and T. J. Rowland, Acta Metallurgica **1,** 731 (1953); T. J. Rowland, Phys. Rev. **119,** 900 (1960).
[102] G. Grüner and M. Minier, Adv. Phys. **26,** 231 (1977).
[103] G. Grüner and M. Minier, Ref. [102]. For references prior to 1977 see P. L. Sagalyn and M. N. Alexander, Phys. Rev. **B 15,** 5581 (1977).
[104] See Table IV of E. N. Kaufmann and R. J. Vianden, Ref. [90].
[105] W. Bartsch, W. Leitz, H. E. Mahnke, W. Semmler, R. Sielemann, and Th. Wickert, in contributed papers volume of the "International Conference on Hyperfine Interactions Studied in Nuclear Reactions and Decay" (E. Karlsson and R. Wäppling, eds.), Uppsala 1974, page 216.
[106] See E. N. Kaufmann and R. J. Vianden, Ref. [90], page 205 for references to the various measurements on ^{117}In ($I = 3/2$) nuclear excited state in Cd metal.
[107] See E. N. Kaufmann and R. J. Vianden, Table IV for references to various measurements on ^{113}Sn ($I = 11/2$) in Cd metal.
[108] O. Hartmann, E. Karlsson, L. O. Norlin, D. Richter, and T. O. Niinkioski, Phys. Rev. Lett. **41,** 1055 (1978).
[109] M. Camani, F. Gygax, F. N. Ruegg, A. Schenck, and H. Schilling, Phys. Rev. Lett. **39,** 836 (1977).
[110] M. Minier, R. Andreani, and C. Minier, Phys. Rev. **B 18,** 102 (1978); see also G. Grüner and M. Minier, Ref. [102].
[111] See for instance P. L. Sagalyn and J. A. Hofmann, Phys. Rev. **127,** 68 (1962) and E. P. Jones and D. L. Williams, Phys. Lett. **1,** 109 (1962) for use of single-crystal techniques with conventional NMR involving higher sensitivity NMR spectrometers for metallic systems.
[112] See for instance, A. G. Redfield, Phys. Rev. **130,** 589 (1963).
[113] P. H. Citrin, P. Eisenberger, and J. E. Rowe, Phys. Rev. Lett. **48,** 802 (1982).
[114] J. Friedel, Phil. Mag. **43,** 153 (1952); Adv. Physics **3,** 446 (1954); Suppl. Nuovo Cim. **2,** 287 (1958).
[115] W. Kohn and S. H. Vosko, Phys. Rev. **119,** 912 (1960).
[116] A. Blandin and J. Friedel, J. Phys. Chem. Sol. **17,** 170 (1960); J. Phys. Radium Paris **21,** 689 (1960).
[117] L. C. R. Alfred and D. O. Van Ostenburg, Phys. Lett. **A 26,** 27 (1969).

[118] B. L. Jensen, R. Nevald, and D. L. Williams, J. Phys. **F 2,** 169 (1972); see Ref. 19 of P. L. Sagalyn and M. N. Alexander, Phys. Rev. **B 15,** 5581 (1977), for correction to Jensen, Neval and Williams' paper.
[119] Y. Fukai and K. Watanabe, Phys. Rev. **B 2,** 2353 (1970); Phys. Rev. **B 10,** 3015 (1974).
[120] M. Manninen, R. Nieminen, P. Hautojärvi, and J. Arponen, Phys. Rev. **B 12,** 4012 (1975).
[121] P. Jena, S. G. Das, and K. G. Singwi, Phys. Rev. Lett. **40,** 264 (1978).
[122] M. Manninen and R. M. Nieminen, J. Phys. **F 9,** 1333 (1979).
[123] M. J. Ponnambalam and P. Jena, Phys. Rev. Lett. **46,** 610 (1981); Solid State Comm. **52,** 411 (1984).
[124] S. D. Raj, J. Singh, and S. Prakash, J. Phys. **F 12,** 1941 (1982).
[125] P. L. Sagalyn, A. Paskin, and R. J. Harrison, Phys. Rev. **124,** 428 (1961).
[126] E. A. Faulkner, Phil. Mag. **5,** 843 (1960).
[127] B. Pal, S. Mahajan, S. D. Raj, J. Singh, and S. Prakash, Phys. Rev. **B 30,** 3191 (1984).
[128] S. Hafizuddin and N. C. Mohapatra, Phys. Lett. **101 A,** 419 (1984).
[129] P. L. Sagalyn and M. N. Alexander, Phys. Rev. **B 15,** 5581 (1977).
[130] L. D. Landau and E. M. Lifshitz, Quantum Mechanics-Non-Relativistic Theory, Pergamon Press, Bristol 1965, page 479.
[131] K. K. P. Rao and N. C. Mohapatra, Phys. Rev. **B 22,** 3767 (1980).
[132] K. K. P. Rao, N. C. Mohapatra, and S. Hafizuddin, Phys. Rev. **B 24,** 1941 (1981).
[133] M. J. Ponnambalam and P. Jena, Hyperfine Inter. **20,** 65 (1984).
[134] Y. Fukai and K. Watanabe (1970), Ref. [119], page 2356.
[135] M. Ponnambalam and P. Jena, Hyperfine Inter. **20,** 65 (1984).
[136] M. J. Ponnambalam and P. Jena (1984), Ref. [123].
[137] C. O. Almbladh and U. von Barth, Phys. Rev. **B 13,** 3307 (1976).
[138] S. D. Mahanti, T. Lee, D, Ikenberry, and T. P. Das, Phys. Rev. **A 9,** 2238 (1974).
[139] T. P. Das, Relativistic Quantum Mechanics of Electrons, Harper and Row, New York 1973, Appendix to Chapter 7.
[140] M. J. Ponnambalam and P. Jena (1981), Ref. [123].
[141] J. D. Eshelby, Advances in Solid State Physics, (F. Seitz and D. Turnbull, eds.), Academic Press, New York 1956, Vol. **3,** page 79.
[142] S. P. Timoshenko and J. N. Goodier, Theory of Elasticity, McGraw Hill, New York 1970.
[143] S. P. Singhal, Phys. Rev. **B 8,** 364 (1973).
[144] F. Perrot and M. Rasolt, Solid State Commun. **36,** 579 (1980).
[145] M. J. Puska and R. M. Nieminen, Phys. Rev. **B 29,** 5382 (1984).
[146] P. C. Schmidt, A. Coker, and T. P. Das, to be published. Preliminary report at International Conference on Hyperfine Interactions Berlin, July 1980.
[147] F. J. Blatt, Phys. Rev. **108,** 285 (1957).
[148] C. M. Hurd and E. M. Gordon, J. Phys. Chem. Sol. **29,** 2205 (1968).
[149] A. Schenck, Muon Spin Rotation Spectroscopy, Adam Hilger, Bristol, 1985.
[150] G. A. Burdick, Phys. Rev. **129,** 138 (1963).
[151] W. M. Shyu, G. D. Gaspari, and T. P. Das, Phys. Rev. **152,** 270 (1966).
[152] Y. Fukai and K. Watanabe (1974), Ref. [119]
[153] P. M. Holtham and P. Jena, J. Phys. **F 5,** 1649 (1975).
[154] The valence contributions in Table 3 are obtained by multiplying the values for Al and Cu in Ref. [136] by the ratios of our $\alpha(k_F)$ in Eqs. (60) and (61) to those assumed in Ref. [136], the value for $\alpha(k_F)$ used for Al in the latter case being the average of the three values obtained in Ref. [153] for the three different choices of pseudopotentials used there.
[155] In Ref. [128], a part of the valence contribution is included with the size effect (private communication with Dr. N. C. Mohapatra and also explained in a forthcoming paper by the authors of Ref. [128] in J. Phys. F (1986)) making the size and valence effects comparable. However, when the valence and size effect contributions are grouped in the same manner as in the authors' earlier work (Ref. [132]) the valence contributions come out rather small compared with the size effect results.
[156] S. R. D. Groot et al., Ref. [5]; P. T. Callaghan et al., Ref. [5]; G. Kaindl et al., Ref. [5].
[157] H. Ackermann et al., Ref. [4].
[158] H. J. Behrend and D. Budnick, Ref. [3].
[159] R. S. Raghavan et al., Ref. [69].
[160] P. C. Pattnaik et al., Ref. [46].
[161] M. D. Thompson et al., Ref. [46].
[162] E. N. Kaufmann and R. J. Vianden, Ref. [90]; see also Proceedings of Sixth International Conference on Hyperfine Interactions, Grönningen, Netherlands, August 1983, in Hyperfine Interactions (1984).
[163] R. S. Raghavan, P. Raghavan, and E. N. Kaufmann, Phys. Rev. Lett. **31,** 111 (1973); erratum **31,** 802 (1973).
[164] P. Raghavan et al., Ref. [56].
[165] M. Thompson, Ref. [48]; M. D. Thompson et al., Ref. [48].
[166] N. C. Mohapatra, T. P. Das, R. M. Sternheimer, and D. Ikenberry, unpublished.
[167] R. M. Sternheimer, Phys. Rev. **159,** 266 (1967).
[168] The choice of HF wave-functions for cores of neutral Zn and In for the γ_∞ calculations in Ref. [166] is desirable for the reason stated in Ref. [70], namely, the shielding of the Zn^{2+} and In^{3+} cores by the conduction electron distribution around them.
[169] F. D. Feiock and W. R. Johnson, Phys. Rev. **187,** 39 (1969).
[170] The value of $Q = 0.57$ barns refers to the ^{67}Zn ($I = 9/2$) excited state and is obtained by using the ratio of the NQCC of 49.5 MHz for this state in the metal (H. Bertschat, E. Recknagel, and B. Spellmayer, Phys. Rev Lett. **34,** 1280 (1975)) to the average NQCC for ^{67}Zn ($I = 5/2$) ground state (Ref. [64–67]) 12.9 MHz and Q of this latter state. The value of Q for ^{67}Zn ($I = 9/2$) is in good agreement with the value of (0.50 ± 0.08) barns obtained from the theoretical value of the EFG calculated by N. C. Mohapatra et al., Ref. [53].
[171] See E. N. Kaufmann and R. J. Vianden, Ref. [90], page 208.
[172] See E. N. Kaufmann and R. J. Vianden, Ref. [90], list following Table IV.
[173] C. M. Singal and T. P. Das, Phys. Rev. **B 8,** 3675 (1973); **B 12,** 795 (1975).
[174] S. N. Ray, T. Lee, and T. P. Das, Phys. Rev. **B 8,** 5291 (1973); M. Vajed-Samii, S. N. Ray, and T. P. Das, Phys. Rev. **B 12,** 4591 (1975).
[175] D. Fick, B. Horn, E. Koch, and W. Memmert, Z. Naturforsch. **41 a,** 113 (1986).
[176] J. C. Browne, Physics Today **29,** 28 (1984); G. C. Fox and S. W. Otto, Physics Today **29,** 50 (1984).